

Seismic moment tensors and estimated uncertainties in southern Alaska

Vipul Silwal and Carl Tape

Journal of Geophysical Research: Solid Earth

March 11, 2016

Contents

| | |
|--|----------|
| S1 ScholarWorks@UA collection | 2 |
| S2 Methods | 2 |
| S2.1 Waveform selection criteria | 2 |
| S2.2 Time shifts | 3 |
| S2.3 Variance Reduction | 3 |
| S3 Results | 4 |
| S3.1 Extended analysis for the example event | 4 |
| S3.2 Two small events | 4 |
| S3.3 Comparison between moment tensor catalogs | 4 |
| References | 5 |

List of Tables

| | |
|---|---|
| S1 scak velocity model | 6 |
| S2 Discretized grid for moment tensor grid search | 6 |
| S3 Comparison tests for Part I catalog | 7 |
| S4 Summary table of detailed analysis | 9 |
| S5 Catalog table as text file | 9 |

List of Figures

| | |
|---|----|
| S1 Southern Alaska seismicity | 10 |
| S2 Data-to-synthetics amplitude ratios | 11 |
| S3 Time-shift plot for example event | 12 |
| S4 Waveform fits for 20071003140612444 for AEC moment tensor | 13 |
| S5 Waveform fits for 20081118195651180 (CAP solution) | 14 |
| S6 Waveform fits for 20081118195651180 at AEC first-motion solution (M_w fixed) | 15 |
| S7 Waveform fits for 20081118195651180 at AEC first-motion solution (M_w search) | 16 |

| | | |
|-----|---|----|
| S8 | Waveform fits for 20090210074254600 at CAP solution | 17 |
| S9 | Waveform fits for 20090210074254600 at AEC first-motion solution | 18 |
| S10 | Waveform fits for 20090210074254600 at AEC first-motion solution | 19 |
| S11 | Extended uncertainty analysis for 20090407201255351 (M_{110}) | 20 |
| S12 | Extended uncertainty analysis for 20090407201255351 (M_{011}) | 21 |
| S13 | Extended uncertainty analysis for 20090407201255351 (M_{101}) | 22 |
| S14 | Extended uncertainty analysis for 20090407201255351 (M_{112}) | 23 |
| S15 | Extended uncertainty analysis for 20090407201255351 (M_{012}) | 24 |
| S16 | Effect of using L2 norm on different data sets for 21 events | 25 |
| S17 | Uncertainty analysis for example 20090407201255351 for M_x | 26 |
| S18 | Uncertainty analysis for example 20090407201255351 for $-M_0$ | 27 |
| S19 | Moment tensors in southern Alaska from various catalogs | 28 |
| S20 | $\omega(M_{\text{CAP}}, M_{\text{AEC}})$ vs ΔVR | 29 |

S1 ScholarWorks@UA collection

Our moment tensor catalog of 106 events is available in the text file in Table S5. We provide the complete results of our analysis in *Silwal* (2015), which includes the following files:

- `scholarworks.pdf` Description of the figures in the collection.
- `PartI_inv.pdf` Waveform fits for 21 Part I catalog events (Table 4). The waveform match is shown for moment tensor M_{111} obtained when using body waves and surface waves at the good stations. (See Section S2.1 for waveform selection criteria and Table 1 for description of moment tensor notations.)
- `PartI_dep.pdf` Depth grid search results for the M_{111} moment tensor inversion for Part I events.
- `PartI_unc.pdf` Uncertainty analysis for the M_{111} moment tensor inversion for Part I events.
- `PartII_inv.pdf` Waveform fits for all 85 events in Part II catalog.
- `input_weight_files.zip` Input weight files for all 21 Part I catalog events.

S2 Methods

S2.1 Waveform selection criteria

As we demonstrated in Section 2.4 and Figure 12, the use of the L1 norm in the misfit function greatly reduces the need to exclude bad waveforms. (By “bad,” we mean that there are errors associated with data gaps or station metadata. Waveforms that are complex due to 3D structure are not considered bad.) For all inversions (except for case M_{110} , for which all waveforms were used) we use waveform selection criteria based on amplitude anomalies, $\ln(A_{\text{obs}}/A_{\text{syn}})$, where A is the maximum value of the waveform within the time window, either for data or synthetics. The five time windows are vertical P (PV), radial P (PR), vertical Rayleigh (SurfZ), radial Rayleigh (SurfR), and transverse Love (SurfT). Our criteria were:

1. Turn off PV and PR if the amplitude ratio of either one exceeds 2.5.

Both PV and PR need to be either ON (weight=1) or OFF (weight=0) together. In other words, we prefer not to use any P waveform if we can only fit it on a single component.

2. Turn off SurfV and SurfR if the amplitude ratio of either one exceeds 1.5.

Both SurfV and SurfR need to be either ON (weight=1) or OFF (weight=0) together. In other words, we prefer not to use any Rayleigh waveform if we can only fit it on a single component.

3. Turn off SurfT if the amplitude ratio exceeds 1.5.

Figure S2 shows how we established the threshold amplitude ratio values. Our motivation was to remove the largest amplitude outliers, since it is possible that these could influence the outcome of the inversions, which use a waveform difference (i.e., based on amplitudes) for the misfit function.

S2.2 Time shifts

Time shifts between data and synthetics are useful in assessing the quality of the 1D velocity model. The maximum allowable time shift is ± 2 s for body waves and ± 10 s for surface waves; we assume that any measured time shift outside these limits is an artifact due to cycle skipping between data and synthetics. The measured time shifts can be represented on a spatial map, with each source-station path colored according to the time shift (Figure S3). In Figure S3 we see a systematic variation in time shifts as a function of station azimuth. Similar plots of time shifts for other time windows (PV, PR, SurfT) and cross-correlation values for all time windows are useful in assessing the quality of the waveform fits between data and synthetics.

S2.3 Variance Reduction

In our study we use probability density $p(M)$ (Eq. 10) as part of our assessment of the quality of our moment tensor solutions. In the published literature, moment tensor solutions are often assessed in terms of their variance reduction. The CAP code of *Zhu and Helmberger* (1996) uses a misfit function based on an L2 norm (Eq. 5). In our study we use an L1 norm (Eq. 4). For each of these norms we calculate variance reduction as:

$$VR_{L1}(M) = 100 \times \left(1 - \left(\frac{\Phi_{L1}(M)}{u_{L1}} \right)^2 \right) \quad (\text{S1})$$

$$VR_{L2}(M) = 100 \times \left(1 - \frac{\Phi_{L2}(M)}{u_{L2}} \right) \quad (\text{S2})$$

where

$$u_{L1} = \sum_{j=1}^{N_s} \sum_{i=1}^5 [\mathbf{u}_{ij}^T \mathbf{W}_{ij} \mathbf{u}_{ij}]^{1/2} \quad (\text{S3})$$

$$u_{L2} = \sum_{j=1}^{N_s} \sum_{i=1}^5 \mathbf{u}_{ij}^T \mathbf{W}_{ij} \mathbf{u}_{ij} \quad (\text{S4})$$

VR is represented as a percentage and varies from $-\infty$ to 100%, with 100% being a perfect fit between data and synthetics. A negative variance reduction can occur when the misfit norm in the numerator is larger than the data norm in the denominator.

S3 Results

S3.1 Extended analysis for the example event

For the example event 20090407201255351 we performed a suite of inversions for different subsets of data ($(M_{111}, M_{110}, M_{011}, M_{101}, M_{112}, M_{012})$; see Table 1 for description). The uncertainty analysis for M_{111} (obtained using body and surface waves at selected stations) is shown in Figure 5; for the rest see Figures S11–S15. These figures show how the confidence measure \mathcal{P}_{AV} changes with the choice of data used.

See Tables S3 and S4 for the summarized results of a similar analysis of all 21 Part I catalog events.

S3.2 Two small events

Among the 85 Part II events, 20081118195651180 had the largest difference ($\omega = 70^\circ$) from the solution in the AEC first-motion catalog (see Figures S5–S7). For the identical misfit function (same set of waveforms), the variance reduction is higher for the CAP solution than for the AEC solution (60 vs 29). This shows that either the body waves or the MOOS stations—neither of which were used in the AEC first-motion solution—are probably very important in estimating this moment tensor. Our magnitude estimate of M_w 4.0 is much higher than the magnitude from the AEC catalog (M_w 3.5).

Figures S8–S10 provides a second example of a small event. The difference between our preferred CAP solution and the AEC first-motion solution is $\omega = \angle(M_{111}, M_{fm}) = 68^\circ$. The variance reduction is better for the CAP solution (38 vs 31), and the body waves fit better. However the comparison shows the challenges associated with moment tensor inversions for events with lower signal-to-noise ratios (like smaller events): the waveform fits for two very different moment tensors appear to be qualitatively comparably good. An uncertainty analysis would benefit these events, as would a detailed investigation of the inclusion of first-motion polarities along with the waveforms.

S3.3 Comparison between moment tensor catalogs

Figure S19 shows maps of different moment tensor catalogs. Figure S20 compares our moment tensors M_{CAP} with those from the AEC moment tensor catalog M_{AEC} . The x -axis shows the decrease in variance reduction for M_{AEC} relative to M_{CAP} . To make the comparison as fair as possible, we allowed the magnitude m_{AEC} to vary when calculating VR ; these are the blue points in Figure S20. The plot shows a correlation between the decrease in variance reduction and the angular difference $\omega = \angle(M_{CAP}, M_{AEC})$, with one event having $\omega = 55^\circ$ and $\Delta VR = 25$ (see Figures 10 and 11).

References

- Ekström, G., M. Nettles, and A. M. Dziewoński (2012), The global GCMT project 2004–2010: Centroid-moment tensors for 13,017 earthquakes, *Phys. Earth Planet. Inter.*, 200–201, 1–9, doi:10.1016/j.pepi.2012.04.002.
- Kanamori, H. (1977), The energy release in great earthquakes, *J. Geophys. Res.*, 82, 2981–2987.
- Lahr, J. C. (1975), Detailed seismic investigation of Pacific-North American plate interaction in southern Alaska, *Ph. D. Thesis, Columbia University*, p. 88.
- Matumoto, T., and R. A. Page (1964), Microaftershocks following the alaska earthquake of 28 march 1964: Determination of hypocenters and crustal velocities in the kenai peninsula-prince william sound area, the prince william sound, alaska, earthquake of 1964 and aftershocks, *U.S. Govt. Printing Office, Washington*, 10(3), 157–173.
- Ratchkovski, N. A., and R. A. Hansen (2002), New constraints on tectonics of interior Alaska: Earthquake locations, source mechanisms, and stress regime, *Bull. Seis. Soc. Am.*, 92(3), 998–1014, doi:10.1785/0120010182.
- Silver, P. G., and T. H. Jordan (1982), Optimal estimation of scalar seismic moment, *Geophys. J. R. Astron. Soc.*, 70, 755–787.
- Silwal, V. (2015), Seismic moment tensor catalog for southern Alaska, ScholarWorks@UA at <http://hdl.handle.net/11122/6025> (last accessed 2016/01/22): descriptor file, text file of catalog, figures with waveform fits, depth searches, and uncertainty analyses.
- Tape, W., and C. Tape (2012), A geometric setting for moment tensors, *Geophys. J. Int.*, 190, 476–498, doi:10.1111/j.1365-246X.2012.05491.x.
- Zhu, L., and D. Helmberger (1996), Advancement in source estimation techniques using broad-band regional seismograms, *Bull. Seis. Soc. Am.*, 86(5), 1634–1641.

Table S1: 1D structural model **sca**k used for generating Green's functions for the moment tensor inversions (*Matumoto and Page*, 1964; *Lahr*, 1975).

| top of layer, km | bottom of layer, km | thickness km | V_S m/s | V_P m/s | density kg/m ³ | Q_S | Q_P |
|------------------|---------------------|--------------|-----------|-----------|---------------------------|-------|-------|
| 0 | 4 | 4 | 3010 | 5300 | 2520 | 300 | 600 |
| 4 | 9 | 5 | 3180 | 5600 | 2610 | 300 | 600 |
| 9 | 14 | 5 | 3520 | 6200 | 2780 | 300 | 600 |
| 14 | 19 | 5 | 3920 | 6900 | 2970 | 300 | 600 |
| 19 | 24 | 5 | 4200 | 7400 | 3120 | 300 | 600 |
| 24 | 33 | 9 | 4370 | 7700 | 3200 | 300 | 600 |
| 33 | 49 | 16 | 4490 | 7900 | 3260 | 300 | 600 |
| 49 | 66 | 17 | 4600 | 8100 | 3320 | 300 | 600 |
| 66 | — | — | 4720 | 8300 | 3370 | 300 | 600 |

Table S2: Discretized grid for moment tensor grid search. NPTS is the number of search points for each interval. m_{AEC} is the magnitude listed in the AEC seismicity catalog. By using the cosine of dip θ we achieve uniform orientations. The depth range listed is representative; when needed, we used a wider search range and a finer (1 km) increment (see *Silwal*, 2015).

| parameter | min | max | interval | | NPTS | |
|--|-----------------|-----------------|---------------|--------------|---------------|--------------|
| | | | (m varies) | (m fixed) | (m varies) | (m fixed) |
| depth z | $z_{AEC} - 20$ | $z_{AEC} + 20$ | 2 km | — | 21 | 0 |
| magnitude m | $m_{AEC} - 0.5$ | $m_{AEC} + 0.5$ | 0.1 | — | 11 | 0 |
| strike κ | 0° | 360° | 10 | 5 | 36 | 72 |
| rake σ | -90° | 90° | 10 | 5 | 19 | 37 |
| cos(dip) $h = \cos \theta$ | 0 | 1 | 0.1 | 0.05 | 9 | 18 |
| total number of points (magnitude and depth fixed) | | | | | 1,422,036 | 47,952 |

Table S3: Summary of inversions for 21 high-quality events when the inversion is performed using the L1 norm. The subtable for 20090407201255351 is in Table 3. The number ω is the angular distance of the corresponding moment tensor from M_{111} . Since M_{AEC} and M_{fm} are obtained from the AEC catalog, neither a waveform match (VR) nor an uncertainty analysis (\mathcal{P}_{AV}) was performed.

| Misfit (see Table 1) | depth km | M_w | ω deg | $p(M_0)$ | \mathcal{P}_{AV} | Misfit (see Table 1) | depth km | M_w | ω deg | $p(M_0)$ | \mathcal{P}_{AV} | | |
|-----------------------------|------------------|-------|-----------------|----------|---------------------------|-------------------------|-------------|------------------|-----------------|----------|---------------------------|-------|------|
| Event 20070911234634153 (1) | | | | | | | | | | | | | |
| L1 | M_{111} | 94 | 4.4 | — | 3.19 | 0.89 | L1 | M_{111} | 69 | 4.9 | — | 7.65 | 0.97 |
| L1 | M_{110} | 94 | 4.4 | 0 | 0.12 | 0.56 | L1 | M_{110} | 83 | 4.9 | 29 | 1.02 | 0.80 |
| L1 | M_{011} | 90 | 4.4 | 16 | 10.85 | 0.99 | L1 | M_{011} | 73 | 4.9 | 0 | 19.03 | 0.98 |
| L1 | M_{101} | 94 | 4.4 | 0 | 1.31 | 0.80 | L1 | M_{101} | 61 | 4.9 | 12 | 3.53 | 0.84 |
| L1 | M_{112} | 122 | 4.5 | 37 | 2.80 | 0.85 | L1 | M_{112} | 71 | 4.9 | 16 | 9.76 | 0.98 |
| L1 | M_{012} | 100 | 4.4 | 15 | 10.04 | 0.98 | L1 | M_{012} | 77 | 4.9 | 0 | 37.40 | 0.99 |
| L1 | M_{AEC} | 100 | 4.4 | 21 | — | — | L1 | M_{AEC} | 75 | 4.8 | 4 | — | — |
| L1 | M_{fm} | 101 | 4.4 | 12 | — | — | L1 | M_{fm} | 70 | 5.0 | 77 | — | — |
| Event 20070919112226549 (2) | | | | | | | | | | | | | |
| L1 | M_{111} | 47 | 4.5 | — | 2.35 | 0.92 | L1 | M_{111} | 139 | 5.1 | — | 8.28 | 0.94 |
| L1 | M_{110} | 39 | 4.4 | 22 | 0.12 | 0.61 | L1 | M_{110} | 143 | 5.0 | 10 | 1.66 | 0.84 |
| L1 | M_{011} | 45 | 4.5 | 18 | 5.72 | 0.97 | L1 | M_{011} | 141 | 5.0 | 50 | 23.07 | 0.99 |
| L1 | M_{101} | 39 | 4.6 | 23 | 0.93 | 0.87 | L1 | M_{101} | 139 | 5.1 | 0 | 6.93 | 0.94 |
| L1 | M_{112} | 57 | 4.6 | 20 | 3.67 | 0.92 | L1 | M_{112} | 137 | 5.1 | 53 | 3.38 | 0.91 |
| L1 | M_{012} | 51 | 4.5 | 31 | 4.52 | 0.97 | L1 | M_{012} | 145 | 5.1 | 43 | 14.12 | 0.95 |
| L1 | M_{AEC} | 35 | 4.4 | 34 | — | — | L1 | M_{AEC} | 165 | 5.0 | 32 | — | — |
| L1 | M_{fm} | 31 | 4.4 | 21 | — | — | L1 | M_{fm} | 144 | 4.9 | 67 | — | — |
| Event 20071003140612444 (3) | | | | | | | | | | | | | |
| L1 | M_{111} | 32 | 5.0 | — | 4.38 | 0.88 | L1 | M_{111} | 65 | 5.1 | — | 1.66 | 0.90 |
| L1 | M_{110} | 32 | 5.0 | 13 | 2.57 | 0.83 | L1 | M_{110} | 67 | 5.1 | 0 | 0.82 | 0.81 |
| L1 | M_{011} | 38 | 5.0 | 62 | 4.46 | 0.95 | L1 | M_{011} | 75 | 5.2 | 8 | 9.15 | 0.98 |
| L1 | M_{101} | 36 | 5.1 | 119 | 3.16 | 0.68 | L1 | M_{101} | 65 | 5.5 | 68 | 0.51 | 0.58 |
| L1 | M_{112} | 26 | 4.9 | 55 | 5.52 | 0.95 | L1 | M_{112} | 63 | 5.0 | 19 | 1.98 | 0.90 |
| L1 | M_{012} | 46 | 5.1 | 61 | 10.43 | 0.98 | L1 | M_{012} | 71 | 5.1 | 8 | 9.69 | 0.98 |
| L1 | M_{AEC} | 40 | 5.2 | 54 | — | — | L1 | M_{AEC} | 75 | 5.3 | 11 | — | — |
| L1 | M_{fm} | 45 | 5.0 | 67 | — | — | L1 | M_{fm} | 69 | 5.3 | 19 | — | — |
| Event 20071010180326301 (4) | | | | | | | | | | | | | |
| L1 | M_{111} | 27 | 4.2 | 0 | 1.56 | 0.90 | L1 | M_{111} | 54 | 4.2 | — | 4.36 | 0.95 |
| L1 | M_{110} | 25 | 4.2 | 10 | 0.23 | 0.63 | L1 | M_{110} | 48 | 4.1 | 0 | 0.08 | 0.56 |
| L1 | M_{011} | 37 | 4.3 | 7 | 8.07 | 0.99 | L1 | M_{011} | 56 | 4.2 | 10 | 16.03 | 0.99 |
| L1 | M_{101} | 29 | 4.4 | 53 | 2.85 | 0.77 | L1 | M_{101} | 40 | 4.3 | 14 | 5.82 | 0.92 |
| L1 | M_{112} | 45 | 4.3 | 41 | 4.80 | 0.95 | L1 | M_{112} | 56 | 4.2 | 19 | 13.52 | 0.96 |
| L1 | M_{012} | 45 | 4.3 | 41 | 11.53 | 0.99 | L1 | M_{012} | 56 | 4.2 | 19 | 28.88 | 0.99 |
| L1 | M_{AEC} | 15 | 4.1 | 19 | — | — | L1 | M_{AEC} | 50 | 4.1 | 14 | — | — |
| L1 | M_{fm} | 12 | 4.0 | 20 | — | — | L1 | M_{fm} | 43 | 4.1 | 13 | — | — |
| Event 20080314093821771 (6) | | | | | | | | | | | | | |
| L1 | M_{111} | 139 | 5.1 | — | 8.28 | 0.94 | L1 | M_{111} | 143 | 5.0 | 10 | 1.66 | 0.84 |
| L1 | M_{110} | 141 | 5.0 | 50 | 23.07 | 0.99 | L1 | M_{110} | 141 | 5.0 | 50 | 23.07 | 0.99 |
| L1 | M_{011} | 139 | 5.1 | 0 | 6.93 | 0.94 | L1 | M_{011} | 139 | 5.1 | 0 | 6.93 | 0.94 |
| L1 | M_{101} | 137 | 5.1 | 53 | 3.38 | 0.91 | L1 | M_{101} | 137 | 5.1 | 53 | 3.38 | 0.91 |
| L1 | M_{112} | 145 | 5.1 | 43 | 14.12 | 0.95 | L1 | M_{112} | 145 | 5.1 | 43 | 14.12 | 0.95 |
| L1 | M_{012} | 165 | 5.0 | 32 | — | — | L1 | M_{012} | 165 | 5.0 | 32 | — | — |
| L1 | M_{AEC} | 165 | 5.0 | 67 | — | — | L1 | M_{AEC} | 165 | 5.0 | 67 | — | — |
| L1 | M_{fm} | 144 | 4.9 | 67 | — | — | L1 | M_{fm} | 144 | 4.9 | 67 | — | — |
| Event 20080327230745201 (7) | | | | | | | | | | | | | |
| L1 | M_{111} | 65 | 5.1 | — | 1.66 | 0.90 | L1 | M_{111} | 65 | 5.1 | — | 1.66 | 0.90 |
| L1 | M_{110} | 67 | 5.1 | 0 | 0.82 | 0.81 | L1 | M_{110} | 67 | 5.1 | 0 | 0.82 | 0.81 |
| L1 | M_{011} | 75 | 5.2 | 8 | 9.15 | 0.98 | L1 | M_{011} | 75 | 5.2 | 8 | 9.15 | 0.98 |
| L1 | M_{101} | 65 | 5.5 | 68 | 0.51 | 0.58 | L1 | M_{101} | 65 | 5.5 | 68 | 0.51 | 0.58 |
| L1 | M_{112} | 63 | 5.0 | 19 | 1.98 | 0.90 | L1 | M_{112} | 63 | 5.0 | 19 | 1.98 | 0.90 |
| L1 | M_{012} | 71 | 5.1 | 8 | 9.69 | 0.98 | L1 | M_{012} | 71 | 5.1 | 8 | 9.69 | 0.98 |
| L1 | M_{AEC} | 75 | 5.3 | 11 | — | — | L1 | M_{AEC} | 75 | 5.3 | 11 | — | — |
| L1 | M_{fm} | 69 | 5.3 | 19 | — | — | L1 | M_{fm} | 69 | 5.3 | 19 | — | — |
| Event 20080828231418631 (8) | | | | | | | | | | | | | |
| L1 | M_{111} | 54 | 4.2 | — | 4.36 | 0.95 | L1 | M_{111} | 54 | 4.2 | — | 4.36 | 0.95 |
| L1 | M_{110} | 48 | 4.1 | 0 | 0.08 | 0.56 | L1 | M_{110} | 48 | 4.1 | 0 | 0.08 | 0.56 |
| L1 | M_{011} | 56 | 4.2 | 10 | 16.03 | 0.99 | L1 | M_{011} | 56 | 4.2 | 10 | 16.03 | 0.99 |
| L1 | M_{101} | 40 | 4.3 | 14 | 5.82 | 0.92 | L1 | M_{101} | 40 | 4.3 | 14 | 5.82 | 0.92 |
| L1 | M_{112} | 56 | 4.2 | 19 | 13.52 | 0.96 | L1 | M_{112} | 56 | 4.2 | 19 | 13.52 | 0.96 |
| L1 | M_{012} | 56 | 4.2 | 19 | 28.88 | 0.99 | L1 | M_{012} | 56 | 4.2 | 19 | 28.88 | 0.99 |
| L1 | M_{AEC} | 50 | 4.1 | 14 | — | — | L1 | M_{AEC} | 50 | 4.1 | 14 | — | — |
| L1 | M_{fm} | 43 | 4.1 | 13 | — | — | L1 | M_{fm} | 43 | 4.1 | 13 | — | — |

Table S3 [CONTINUED]:

| Misfit (see Table 1) | depth km | M_w | ω deg | $p(M_0)$ | \mathcal{P}_{AV} | Misfit (see Table 1) | depth km | M_w | ω deg | $p(M_0)$ | \mathcal{P}_{AV} | | |
|------------------------------|-------------|-------|-----------------|----------|--------------------|-------------------------|-------------|-----------|-----------------|----------|--------------------|--------|------|
| Event 20080918194353069 (9) | | | | | | | | | | | | | |
| L1 | M_{111} | 81 | 4.6 | — | 0.88 | 0.78 | L1 | M_{111} | 81 | 4.9 | — | 11.76 | 0.94 |
| L1 | M_{110} | 89 | 4.6 | 19 | 0.08 | 0.54 | L1 | M_{110} | 83 | 4.9 | 10 | 13.38 | 0.95 |
| L1 | M_{011} | 93 | 4.6 | 11 | 2.67 | 0.92 | L1 | M_{011} | 85 | 5.0 | 0 | 28.26 | 0.99 |
| L1 | M_{101} | 79 | 4.7 | 56 | 0.88 | 0.71 | L1 | M_{101} | 103 | 5.3 | 110 | 130.61 | 0.89 |
| L1 | M_{112} | 85 | 4.6 | 151 | 0.93 | 0.51 | L1 | M_{112} | 83 | 4.9 | 0 | 21.56 | 0.99 |
| L1 | M_{012} | 77 | 4.6 | 10 | 13.55 | 0.96 | L1 | M_{012} | 95 | 5.0 | 10 | 41.25 | 0.99 |
| L1 | M_{AEC} | 85 | 4.5 | 8 | — | — | L1 | M_{AEC} | 85 | 4.9 | 26 | — | — |
| L1 | M_{fm} | 90 | 4.7 | 27 | — | — | L1 | M_{fm} | 88 | 4.8 | 25 | — | — |
| Event 20081228071310738 (10) | | | | | | | | | | | | | |
| L1 | M_{111} | 82 | 4.6 | — | 4.28 | 0.95 | L1 | M_{111} | 96 | 4.3 | — | 0.75 | 0.78 |
| L1 | M_{110} | 76 | 4.5 | 18 | 0.16 | 0.60 | L1 | M_{110} | 96 | 4.3 | 31 | 0.04 | 0.52 |
| L1 | M_{011} | 84 | 4.5 | 26 | 24.92 | 0.99 | L1 | M_{011} | 98 | 4.3 | 0 | 9.41 | 0.98 |
| L1 | M_{101} | 90 | 4.7 | 17 | 3.59 | 0.91 | L1 | M_{101} | 120 | 4.5 | 59 | 0.72 | 0.59 |
| L1 | M_{112} | 92 | 4.6 | 21 | 4.42 | 0.97 | L1 | M_{112} | 120 | 4.3 | 55 | 0.23 | 0.57 |
| L1 | M_{012} | 88 | 4.5 | 26 | 32.69 | 0.99 | L1 | M_{012} | 92 | 4.3 | 13 | 6.17 | 0.96 |
| L1 | M_{AEC} | 80 | 4.4 | 25 | — | — | L1 | M_{AEC} | 90 | 4.2 | 17 | — | — |
| L1 | M_{fm} | 89 | 4.5 | 27 | — | — | L1 | M_{fm} | 90 | 4.0 | 19 | — | — |
| Event 20090124180950811 (11) | | | | | | | | | | | | | |
| L1 | M_{111} | 105 | 5.8 | — | 1.33 | 0.85 | L1 | M_{111} | 111 | 4.3 | — | 0.89 | 0.83 |
| L1 | M_{110} | 117 | 5.7 | 10 | 0.71 | 0.72 | L1 | M_{110} | 101 | 4.2 | 10 | 0.06 | 0.56 |
| L1 | M_{011} | 103 | 5.7 | 10 | 14.86 | 0.98 | L1 | M_{011} | 107 | 4.3 | 27 | 2.56 | 0.96 |
| L1 | M_{101} | 109 | 6.0 | 52 | 0.31 | 0.68 | L1 | M_{101} | 115 | 4.6 | 125 | 6.43 | 0.67 |
| L1 | M_{112} | 97 | 5.7 | 20 | 2.14 | 0.93 | L1 | M_{112} | 121 | 4.2 | 50 | 0.24 | 0.60 |
| L1 | M_{012} | 97 | 5.7 | 10 | 9.56 | 0.98 | L1 | M_{012} | 113 | 4.3 | 20 | 31.20 | 0.99 |
| L1 | M_{AEC} | 95 | 5.7 | 30 | — | — | L1 | M_{AEC} | 105 | 4.3 | 24 | — | — |
| L1 | M_{fm} | 98 | 5.9 | 29 | — | — | L1 | M_{fm} | 118 | 4.1 | 21 | — | — |
| Event 20090215193500098 (12) | | | | | | | | | | | | | |
| L1 | M_{111} | 43 | 4.5 | — | 1.80 | 0.93 | L1 | M_{111} | 40 | 4.8 | — | 5.52 | 0.89 |
| L1 | M_{110} | 43 | 4.5 | 0 | 0.86 | 0.84 | L1 | M_{110} | 40 | 4.8 | 0 | 3.88 | 0.85 |
| L1 | M_{011} | 45 | 4.5 | 12 | 4.14 | 0.97 | L1 | M_{011} | 48 | 4.9 | 10 | 5.18 | 0.96 |
| L1 | M_{101} | 55 | 4.5 | 36 | 1.09 | 0.77 | L1 | M_{101} | 62 | 4.6 | 118 | 0.59 | 0.63 |
| L1 | M_{112} | 51 | 4.6 | 17 | 2.61 | 0.95 | L1 | M_{112} | 44 | 4.8 | 28 | 8.80 | 0.91 |
| L1 | M_{012} | 43 | 4.5 | 17 | 7.26 | 0.98 | L1 | M_{012} | 50 | 4.9 | 16 | 4.48 | 0.92 |
| L1 | M_{AEC} | 35 | 4.5 | 25 | — | — | L1 | M_{AEC} | 40 | 4.9 | 25 | — | — |
| L1 | M_{fm} | 37 | 4.3 | 27 | — | — | L1 | M_{fm} | 53 | 4.9 | 65 | — | — |
| Event 20090223000427175 (13) | | | | | | | | | | | | | |
| L1 | M_{111} | 81 | 4.6 | — | 0.88 | 0.78 | L1 | M_{111} | 83 | 4.9 | 10 | 13.38 | 0.95 |
| L1 | M_{110} | 89 | 4.6 | 19 | 0.08 | 0.54 | L1 | M_{110} | 85 | 5.0 | 0 | 28.26 | 0.99 |
| L1 | M_{011} | 93 | 4.6 | 11 | 2.67 | 0.92 | L1 | M_{011} | 103 | 5.3 | 110 | 130.61 | 0.89 |
| L1 | M_{101} | 79 | 4.7 | 56 | 0.88 | 0.71 | L1 | M_{101} | 103 | 5.3 | 110 | 130.61 | 0.89 |
| L1 | M_{112} | 85 | 4.6 | 151 | 0.93 | 0.51 | L1 | M_{112} | 83 | 4.9 | 0 | 21.56 | 0.99 |
| L1 | M_{012} | 77 | 4.6 | 10 | 13.55 | 0.96 | L1 | M_{012} | 95 | 5.0 | 10 | 41.25 | 0.99 |
| L1 | M_{AEC} | 85 | 4.5 | 8 | — | — | L1 | M_{AEC} | 85 | 4.9 | 26 | — | — |
| L1 | M_{fm} | 90 | 4.7 | 27 | — | — | L1 | M_{fm} | 88 | 4.8 | 25 | — | — |
| Event 20090317011333066 (14) | | | | | | | | | | | | | |
| L1 | M_{111} | 96 | 4.3 | — | 0.75 | 0.78 | L1 | M_{111} | 96 | 4.3 | 31 | 0.04 | 0.52 |
| L1 | M_{110} | 98 | 4.3 | 0 | 9.41 | 0.98 | L1 | M_{110} | 98 | 4.3 | 0 | 9.41 | 0.98 |
| L1 | M_{011} | 120 | 4.5 | 59 | 0.72 | 0.59 | L1 | M_{011} | 120 | 4.5 | 59 | 0.72 | 0.59 |
| L1 | M_{101} | 120 | 4.3 | 55 | 0.23 | 0.57 | L1 | M_{101} | 120 | 4.3 | 55 | 0.23 | 0.57 |
| L1 | M_{112} | 92 | 4.3 | 13 | 6.17 | 0.96 | L1 | M_{112} | 92 | 4.3 | 13 | 6.17 | 0.96 |
| L1 | M_{012} | 90 | 4.2 | 17 | — | — | L1 | M_{012} | 90 | 4.2 | 17 | — | — |
| L1 | M_{AEC} | 90 | 4.0 | 19 | — | — | L1 | M_{AEC} | 90 | 4.0 | 19 | — | — |
| L1 | M_{fm} | 90 | 4.1 | 21 | — | — | L1 | M_{fm} | 90 | 4.1 | 21 | — | — |
| Event 20090414171427415 (16) | | | | | | | | | | | | | |
| L1 | M_{111} | 111 | 4.3 | — | 0.89 | 0.83 | L1 | M_{111} | 101 | 4.2 | 10 | 0.06 | 0.56 |
| L1 | M_{110} | 107 | 4.3 | 27 | 2.56 | 0.96 | L1 | M_{110} | 107 | 4.3 | 27 | 2.56 | 0.96 |
| L1 | M_{011} | 115 | 4.6 | 125 | 6.43 | 0.67 | L1 | M_{011} | 115 | 4.6 | 125 | 6.43 | 0.67 |
| L1 | M_{101} | 121 | 4.2 | 50 | 0.24 | 0.60 | L1 | M_{101} | 121 | 4.2 | 50 | 0.24 | 0.60 |
| L1 | M_{112} | 113 | 4.3 | 20 | 31.20 | 0.99 | L1 | M_{112} | 113 | 4.3 | 20 | 31.20 | 0.99 |
| L1 | M_{012} | 105 | 4.3 | 24 | — | — | L1 | M_{012} | 105 | 4.3 | 24 | — | — |
| L1 | M_{AEC} | 118 | 4.1 | 21 | — | — | L1 | M_{AEC} | 118 | 4.1 | 21 | — | — |
| L1 | M_{fm} | 118 | 4.1 | 21 | — | — | L1 | M_{fm} | 118 | 4.1 | 21 | — | — |
| Event 20090430045457938 (17) | | | | | | | | | | | | | |
| L1 | M_{111} | 40 | 4.8 | — | 5.52 | 0.89 | L1 | M_{111} | 40 | 4.8 | 0 | 3.88 | 0.85 |
| L1 | M_{110} | 48 | 4.9 | 10 | 5.18 | 0.96 | L1 | M_{110} | 48 | 4.9 | 10 | 5.18 | 0.96 |
| L1 | M_{011} | 62 | 4.6 | 118 | 0.59 | 0.63 | L1 | M_{011} | 62 | 4.6 | 118 | 0.59 | 0.63 |
| L1 | M_{101} | 44 | 4.8 | 28 | 8.80 | 0.91 | L1 | M_{101} | 44 | 4.8 | 28 | 8.80 | 0.91 |
| L1 | M_{112} | 50 | 4.9 | 16 | 4.48 | 0.92 | L1 | M_{112} | 50 | 4.9 | 16 | 4.48 | 0.92 |
| L1 | M_{012} | 40 | 4.9 | 25 | — | — | L1 | M_{012} | 40 | 4.9 | 25 | — | — |
| L1 | M_{AEC} | 53 | 4.9 | 65 | — | — | L1 | M_{AEC} | 53 | 4.9 | 65 | — | — |
| L1 | M_{fm} | 53 | 4.9 | 65 | — | — | L1 | M_{fm} | 53 | 4.9 | 65 | — | — |

Table S3 [CONTINUED]:

| Misfit (see Table 1) | depth km | M_w | ω deg | $p(M_0)$ | \mathcal{P}_{AV} | Misfit (see Table 1) | depth km | M_w | ω deg | $p(M_0)$ | \mathcal{P}_{AV} | | |
|------------------------------|-------------|-------|-----------------|----------|--------------------|-------------------------|-------------|-----------|-----------------|----------|--------------------|-------|------|
| Event 20090524094004552 (18) | | | | | | | | | | | | | |
| L1 | M_{111} | 109 | 4.6 | — | 2.02 | 0.89 | L1 | M_{111} | 56 | 4.2 | — | 7.72 | 0.95 |
| L1 | M_{110} | 123 | 4.6 | 13 | 0.13 | 0.58 | L1 | M_{110} | 50 | 4.1 | 13 | 0.05 | 0.53 |
| L1 | M_{011} | 125 | 4.7 | 24 | 9.84 | 0.98 | L1 | M_{011} | 54 | 4.2 | 19 | 11.65 | 0.98 |
| L1 | M_{101} | 107 | 4.6 | 0 | 1.12 | 0.82 | L1 | M_{101} | 50 | 4.2 | 10 | 6.74 | 0.75 |
| L1 | M_{112} | 125 | 4.7 | 43 | 2.88 | 0.84 | L1 | M_{112} | 58 | 4.3 | 14 | 10.03 | 0.97 |
| L1 | M_{012} | 129 | 4.7 | 24 | 5.47 | 0.90 | L1 | M_{012} | 56 | 4.2 | 30 | 25.28 | 0.98 |
| L1 | M_{AEC} | 125 | 4.6 | 29 | — | — | L1 | M_{AEC} | 60 | 4.2 | 25 | — | — |
| L1 | M_{fm} | 125 | 4.7 | 27 | — | — | L1 | M_{fm} | 59 | 4.2 | 20 | — | — |
| Event 20090622192805162 (19) | | | | | | | | | | | | | |
| L1 | M_{111} | 62 | 5.4 | — | 4.30 | 0.94 | L1 | M_{111} | 60 | 4.6 | — | 3.62 | 0.94 |
| L1 | M_{110} | 64 | 5.4 | 0 | 2.45 | 0.89 | L1 | M_{110} | 54 | 4.5 | 28 | 0.04 | 0.52 |
| L1 | M_{011} | 62 | 5.4 | 10 | 14.97 | 0.99 | L1 | M_{011} | 60 | 4.6 | 10 | 7.35 | 0.97 |
| L1 | M_{101} | 52 | 5.6 | 24 | 3.04 | 0.66 | L1 | M_{101} | 60 | 4.7 | 29 | 4.33 | 0.89 |
| L1 | M_{112} | 60 | 5.4 | 10 | 6.61 | 0.96 | L1 | M_{112} | 58 | 4.5 | 36 | 4.56 | 0.97 |
| L1 | M_{012} | 60 | 5.4 | 10 | 16.27 | 0.99 | L1 | M_{012} | 58 | 4.5 | 30 | 2.52 | 0.96 |
| L1 | M_{AEC} | 80 | 5.5 | 13 | — | — | L1 | M_{AEC} | 30 | 4.4 | 17 | — | — |
| L1 | M_{fm} | 65 | 5.5 | 13 | — | — | L1 | M_{fm} | 44 | 4.6 | 28 | — | — |
| Event 20090730223910267 (21) | | | | | | | | | | | | | |
| L1 | M_{111} | 60 | 4.6 | — | — | — | L1 | M_{111} | 60 | 4.6 | — | 3.62 | 0.94 |
| L1 | M_{110} | 54 | 4.5 | 28 | — | — | L1 | M_{110} | 54 | 4.5 | 28 | 0.04 | 0.52 |
| L1 | M_{011} | 60 | 4.6 | 10 | — | — | L1 | M_{011} | 60 | 4.6 | 10 | 7.35 | 0.97 |
| L1 | M_{101} | 60 | 4.7 | 29 | — | — | L1 | M_{101} | 60 | 4.7 | 29 | 4.33 | 0.89 |
| L1 | M_{112} | 58 | 4.5 | 36 | — | — | L1 | M_{112} | 58 | 4.5 | 36 | 4.56 | 0.97 |
| L1 | M_{012} | 58 | 4.5 | 30 | — | — | L1 | M_{012} | 58 | 4.5 | 30 | 2.52 | 0.96 |
| L1 | M_{AEC} | 30 | 4.4 | 17 | — | — | L1 | M_{AEC} | 30 | 4.4 | 17 | — | — |
| L1 | M_{fm} | 44 | 4.6 | 28 | — | — | L1 | M_{fm} | 44 | 4.6 | 28 | — | — |

Table S4: An abridged version of the information in Table S3 (and Table 3). Here we exclude the depths and magnitudes and also the values for the AEC moment tensors. We take M_{111} to be the best solution, in the sense that it fits the most waveforms; ω is measured with respect to the M_{111} moment tensor. The column labels are described in Table 1. The data in this table were used in making Figure 14.

| | $p(M_0)$ | | | | | | ω | | | | | | \mathcal{P}_{AV} | | | | | |
|----|----------|-------|-------|--------|-------|-------|----------|-----|-----|-----|-----|-----|--------------------|------|------|------|------|------|
| | 111 | 110 | 011 | 101 | 112 | 012 | 111 | 110 | 011 | 101 | 112 | 012 | 111 | 110 | 011 | 101 | 112 | 012 |
| 1 | 3.19 | 0.12 | 10.85 | 1.31 | 2.80 | 10.04 | — | 0 | 16 | 0 | 37 | 15 | 0.89 | 0.56 | 0.99 | 0.80 | 0.85 | 0.98 |
| 2 | 2.35 | 0.12 | 5.72 | 0.93 | 3.67 | 4.52 | — | 22 | 18 | 23 | 20 | 31 | 0.92 | 0.61 | 0.97 | 0.87 | 0.92 | 0.97 |
| 3 | 4.38 | 2.57 | 4.46 | 3.16 | 5.52 | 10.43 | — | 13 | 62 | 119 | 55 | 61 | 0.88 | 0.83 | 0.95 | 0.68 | 0.95 | 0.98 |
| 4 | 1.56 | 0.23 | 8.07 | 2.85 | 4.80 | 11.53 | — | 10 | 7 | 53 | 41 | 41 | 0.90 | 0.63 | 0.99 | 0.77 | 0.95 | 0.99 |
| 5 | 7.65 | 1.02 | 19.03 | 3.53 | 9.76 | 37.40 | — | 29 | 0 | 12 | 16 | 0 | 0.97 | 0.80 | 0.98 | 0.84 | 0.98 | 0.99 |
| 6 | 8.28 | 1.66 | 23.07 | 6.93 | 3.38 | 14.12 | — | 10 | 50 | 0 | 53 | 43 | 0.94 | 0.84 | 0.99 | 0.94 | 0.91 | 0.95 |
| 7 | 1.66 | 0.82 | 9.15 | 0.51 | 1.98 | 9.69 | — | 0 | 8 | 68 | 19 | 8 | 0.90 | 0.81 | 0.98 | 0.58 | 0.90 | 0.98 |
| 8 | 4.36 | 0.08 | 16.03 | 5.82 | 13.52 | 28.88 | — | 0 | 10 | 14 | 19 | 19 | 0.95 | 0.56 | 0.99 | 0.92 | 0.96 | 0.99 |
| 9 | 0.88 | 0.08 | 2.67 | 0.88 | 0.93 | 13.55 | — | 19 | 11 | 56 | 151 | 10 | 0.78 | 0.54 | 0.92 | 0.71 | 0.51 | 0.96 |
| 10 | 4.28 | 0.16 | 24.92 | 3.59 | 4.42 | 32.69 | — | 18 | 26 | 17 | 21 | 26 | 0.95 | 0.60 | 0.99 | 0.91 | 0.97 | 0.99 |
| 11 | 1.33 | 0.71 | 14.86 | 0.31 | 2.14 | 9.56 | — | 10 | 10 | 52 | 20 | 10 | 0.85 | 0.72 | 0.98 | 0.68 | 0.93 | 0.98 |
| 12 | 1.80 | 0.86 | 4.14 | 1.09 | 2.61 | 7.26 | — | 0 | 12 | 36 | 17 | 17 | 0.93 | 0.84 | 0.97 | 0.77 | 0.95 | 0.98 |
| 13 | 11.76 | 13.38 | 28.26 | 130.61 | 21.56 | 41.25 | — | 10 | 0 | 110 | 0 | 10 | 0.94 | 0.95 | 0.99 | 0.89 | 0.99 | 0.99 |
| 14 | 0.75 | 0.04 | 9.41 | 0.72 | 0.23 | 6.17 | — | 31 | 0 | 59 | 55 | 13 | 0.78 | 0.52 | 0.98 | 0.59 | 0.57 | 0.96 |
| 15 | 3.30 | 0.04 | 9.26 | 2.26 | 2.27 | 10.44 | — | 26 | 9 | 21 | 10 | 10 | 0.95 | 0.52 | 0.98 | 0.77 | 0.95 | 0.98 |
| 16 | 0.89 | 0.06 | 2.56 | 6.43 | 0.24 | 31.20 | — | 10 | 27 | 125 | 50 | 20 | 0.83 | 0.56 | 0.96 | 0.67 | 0.60 | 0.99 |
| 17 | 5.52 | 3.88 | 5.18 | 0.59 | 8.80 | 4.48 | — | 0 | 10 | 118 | 28 | 16 | 0.89 | 0.85 | 0.96 | 0.63 | 0.91 | 0.92 |
| 18 | 2.02 | 0.13 | 9.84 | 1.12 | 2.88 | 5.47 | — | 13 | 24 | 0 | 43 | 24 | 0.89 | 0.58 | 0.98 | 0.82 | 0.84 | 0.90 |
| 19 | 4.30 | 2.45 | 14.97 | 3.04 | 6.61 | 16.27 | — | 0 | 10 | 24 | 10 | 10 | 0.94 | 0.89 | 0.99 | 0.66 | 0.96 | 0.99 |
| 20 | 7.72 | 0.05 | 11.65 | 6.74 | 10.03 | 25.28 | — | 13 | 19 | 10 | 14 | 30 | 0.95 | 0.53 | 0.98 | 0.75 | 0.97 | 0.98 |
| 21 | 3.62 | 0.04 | 7.35 | 4.33 | 4.56 | 2.52 | — | 28 | 10 | 29 | 36 | 30 | 0.94 | 0.52 | 0.97 | 0.89 | 0.97 | 0.96 |

Table S5: [SEPARATE FILE] Text file version of our moment tensor catalog of 106 events, including Part I (Table 4) and Part II. Details can be found within the header lines, which also refer to Kanamori (1977); Silver and Jordan (1982); Tape and Tape (2012).

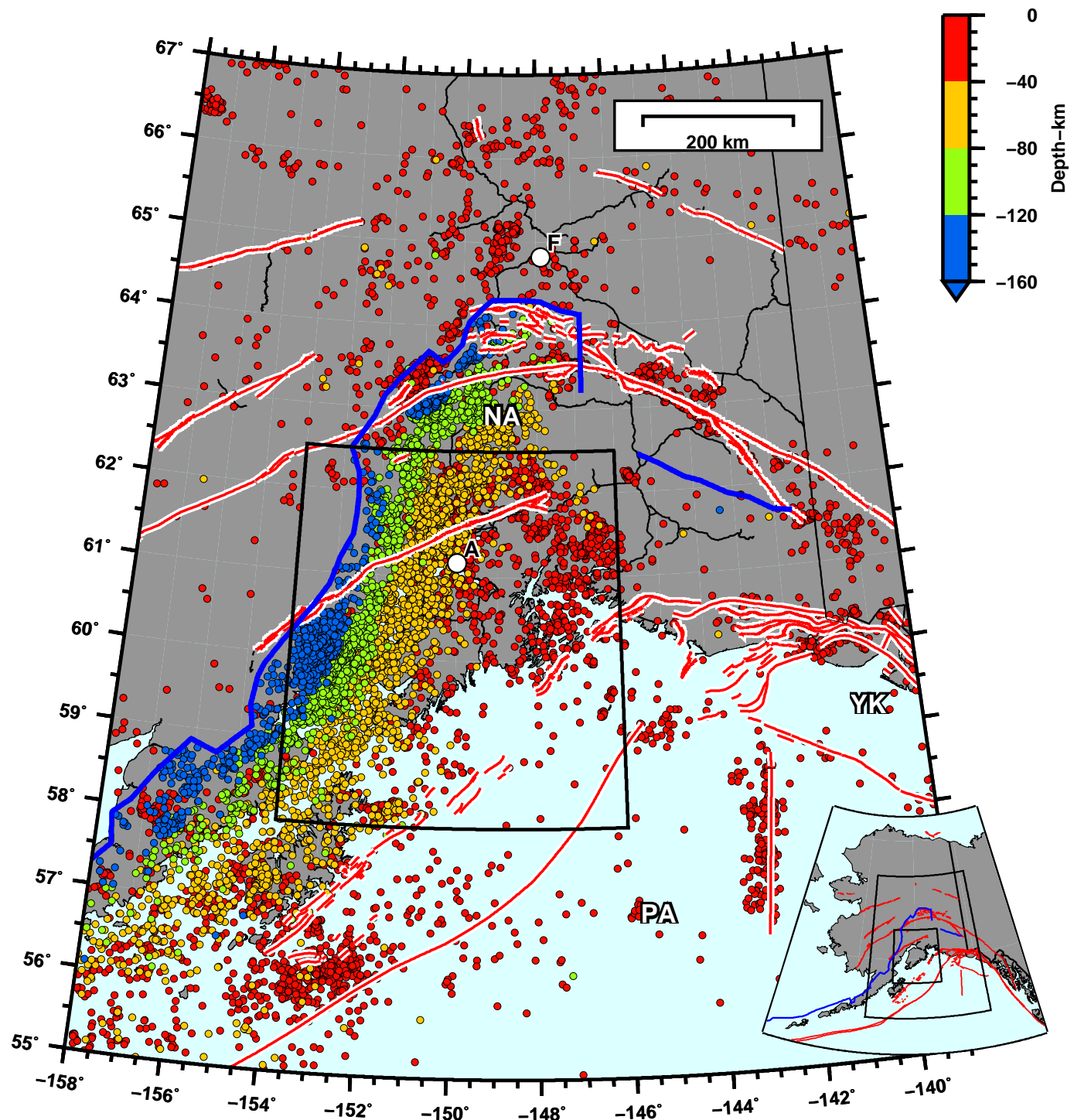


Figure S1: Seismicity in southern Alaska for $M_w \geq 3.0$ between 1990–2014 (source: Alaska Earthquake Center catalog). For caption details, see Figure 1, which also shows the Cook Inlet basement surface (but no seismicity).

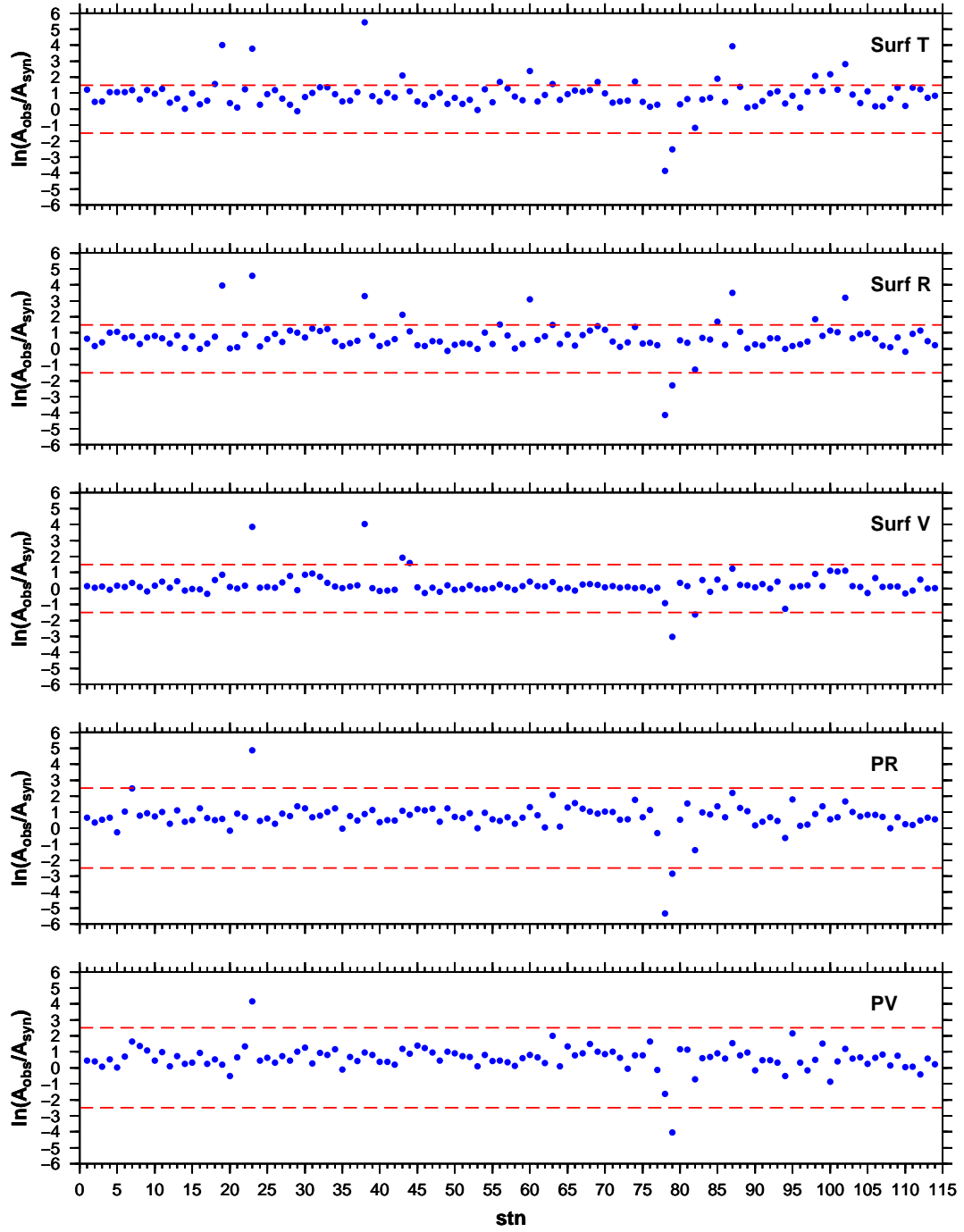


Figure S2: Waveform amplitude ratios between observed data and synthetics, $\ln(A_{\text{obs}}/A_{\text{syn}})$, where A is the max value of the waveform within the time window. Each row represents a different time window used in the moment tensor inversions: P wave vertical component (PV), P wave radial component (PR), Rayleigh wave vertical component (SurfV), Rayleigh wave horizontal component (SurfR), and Love wave transverse component (SurfT). The y -value is the amplitude ratio for a given time window for a given station, averaged over all 21 events (Part I catalog). The x -value is a station index; for the purposes here, what matters is that certain stations are consistent outliers. We use these amplitude ratios to determine threshold levels (red dashed lines) for waveform selection, which are chosen as 2.5 for body waves and 1.5 for surface waves. Waveform selection criteria are listed in Section S2.1.

CAP results for eid 20090407201255351, depth 39 km (catalog 33.0 km)

model scak_039 (strike 200, dip 52.011387, rake -90) Mw 4.50 VR 54.5

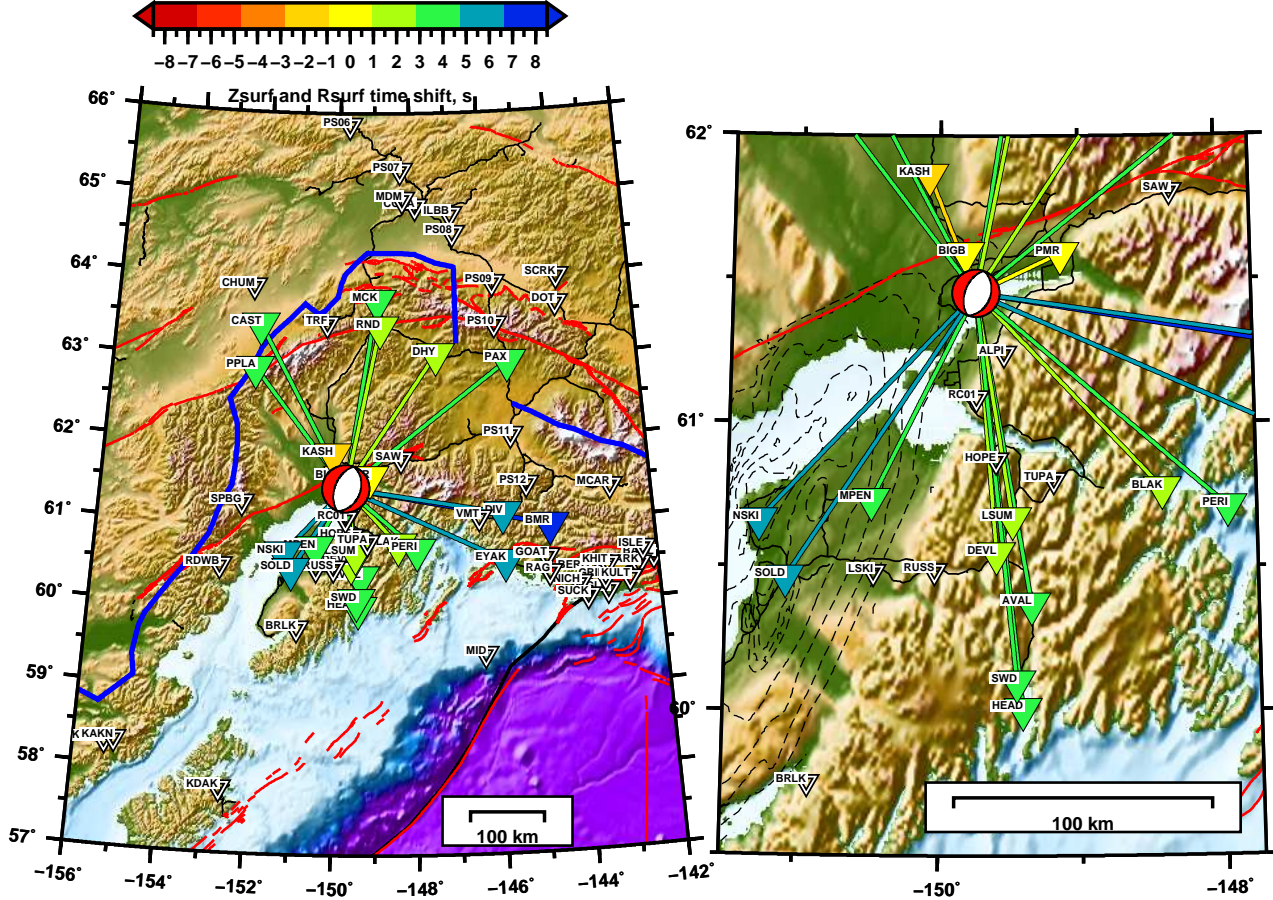


Figure S3: Source-station paths used for event 20090407201255351. The ray paths are colored by the cross correlation time-shift values for the Rayleigh waves (SurfV and SurfR). Notice the large systematic time-shifts (up to +8 seconds) at large distances. Positive time-shifts mean that the synthetic is arriving before the data, i.e., the assumed 1D velocity model is faster than the true Earth model. Notice that the time-shifts to stations toward the southwest, in Cook Inlet basin, are larger than paths in other directions having comparable distances.

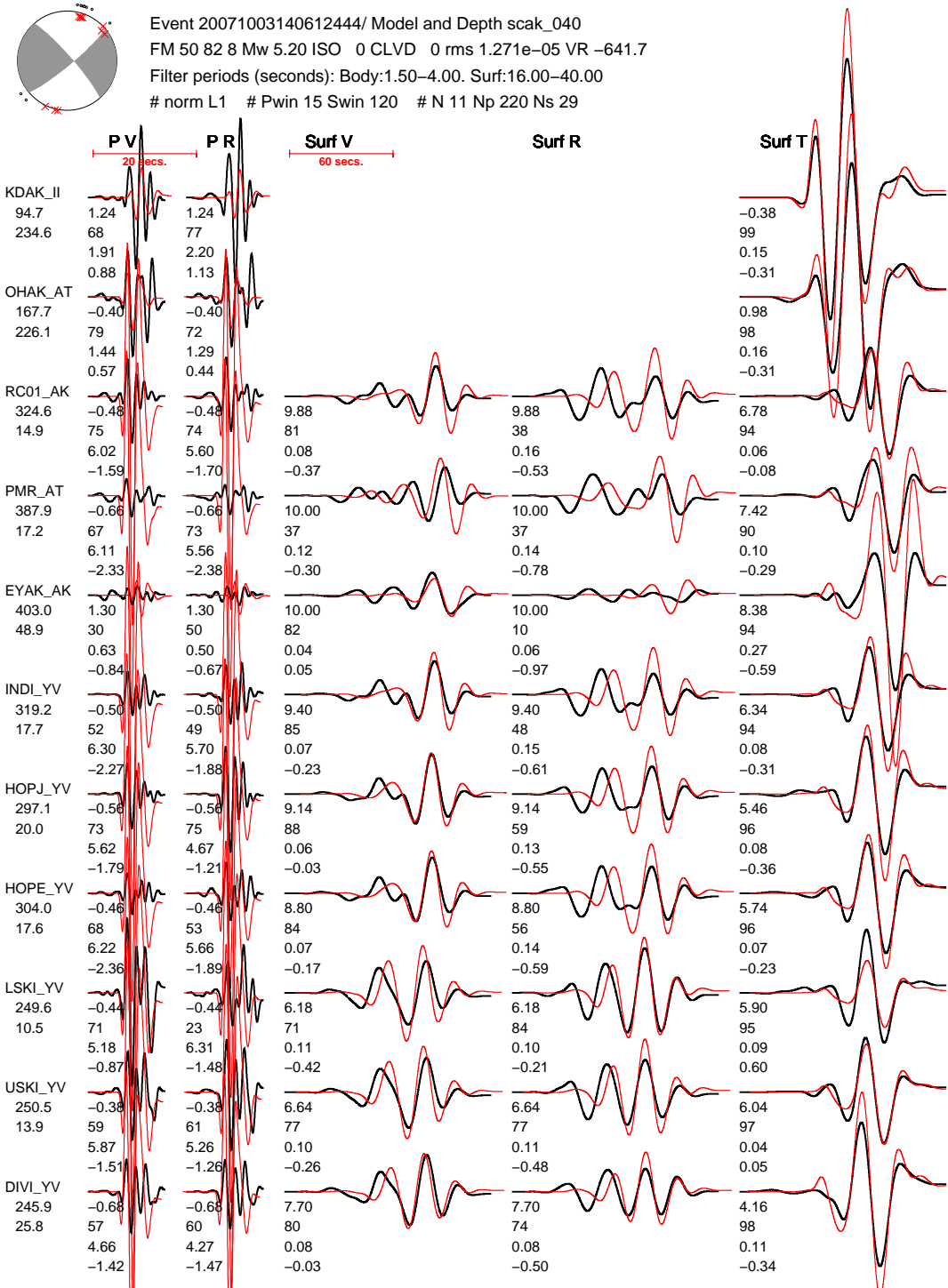


Figure S4: Waveform fits for event 20071003140612444 using the AEC moment tensor solution (fixed orientation, depth, and magnitude M_w 5.2). It is not too surprising that there are poor fits to the body waves, since only long period surface waves were used by AEC for finding their solution. See Figure 10 for our solution obtained using both the body and surface waves, and Figure 11 for waveform fits when we allow the AEC solution to search over magnitude.

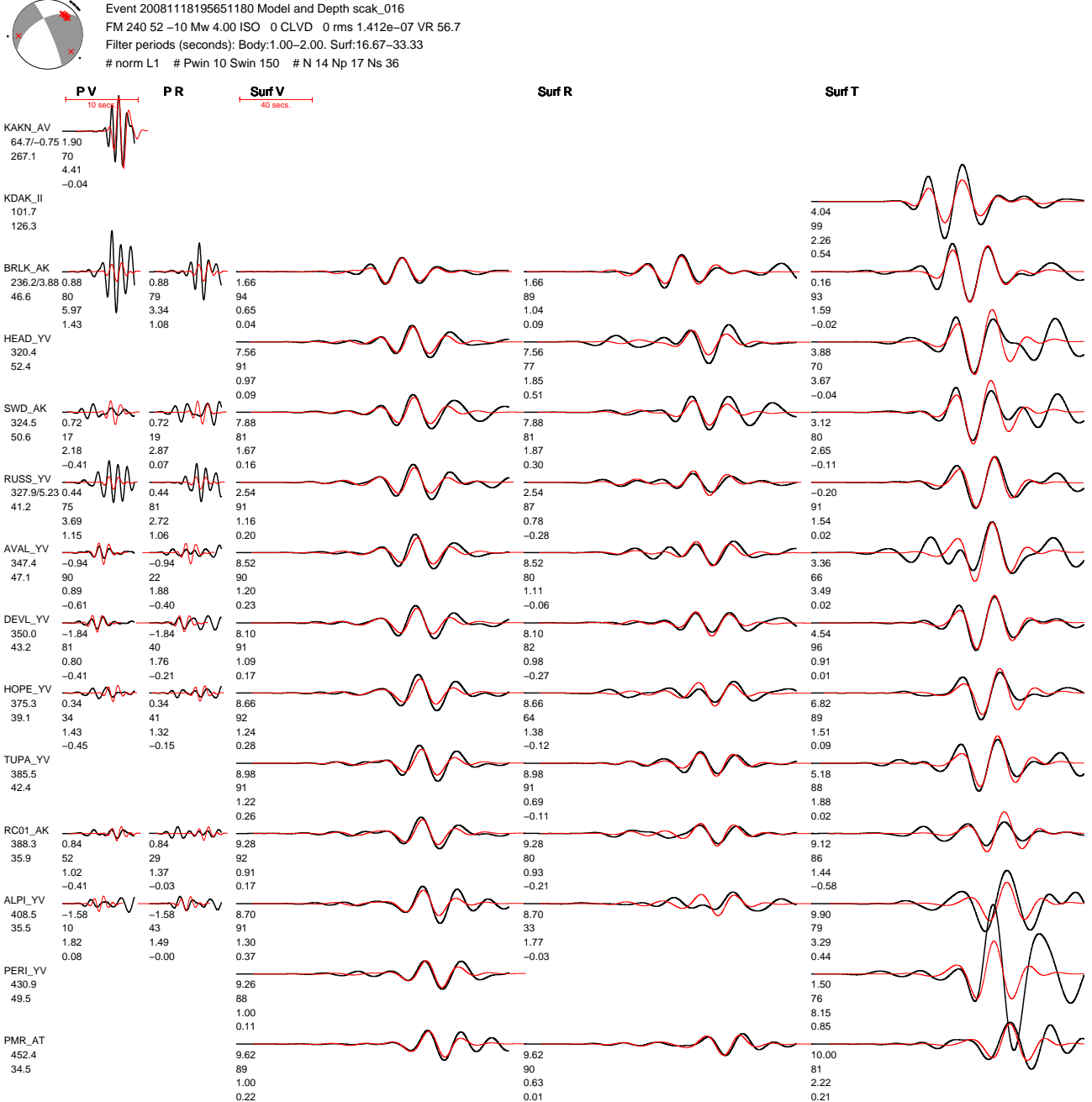


Figure S5: Moment tensor solution and waveform fits for a small magnitude event 20081118195651180 (Table S5). Our magnitude estimate (M_w 4.0) is significantly higher than the AEC catalog (M_w 3.5). See Figure S6 for the waveform fits for the AEC first-motion solution.

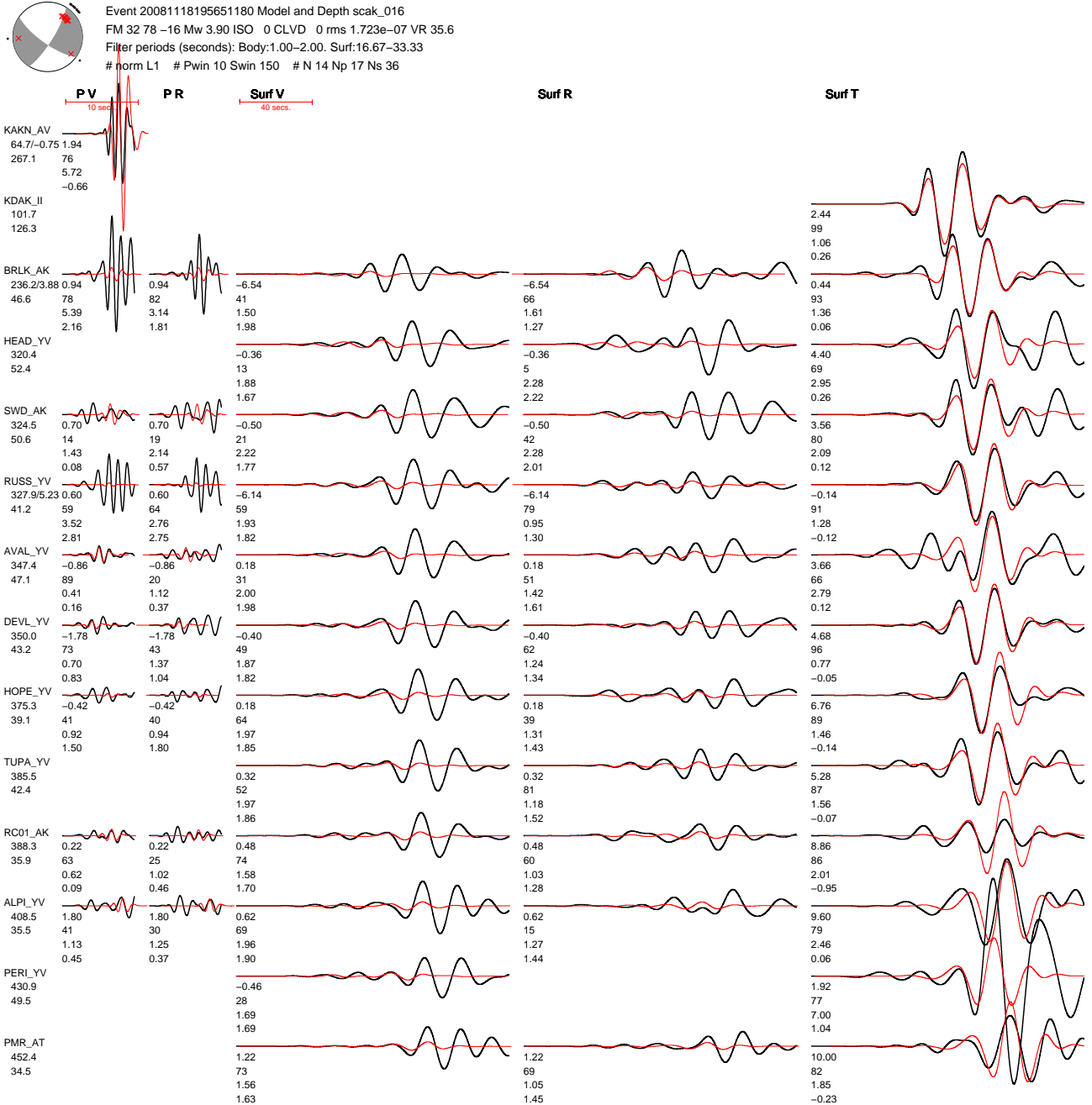


Figure S6: Waveform fits for event 20081118195651180 using the solution from the AEC first-motion catalog. Here we allow the magnitude to vary in order to achieve the best possible waveform fits for this fixed hypocenter and orientation. The magnitude obtained (M_w 3.9) is significantly higher than the AEC catalog magnitude (M_w 3.5). Figure S7 shows the waveform fits when the magnitude is fixed to be the magnitude in the AEC catalog. See Figure S5 for comparison with our solution.

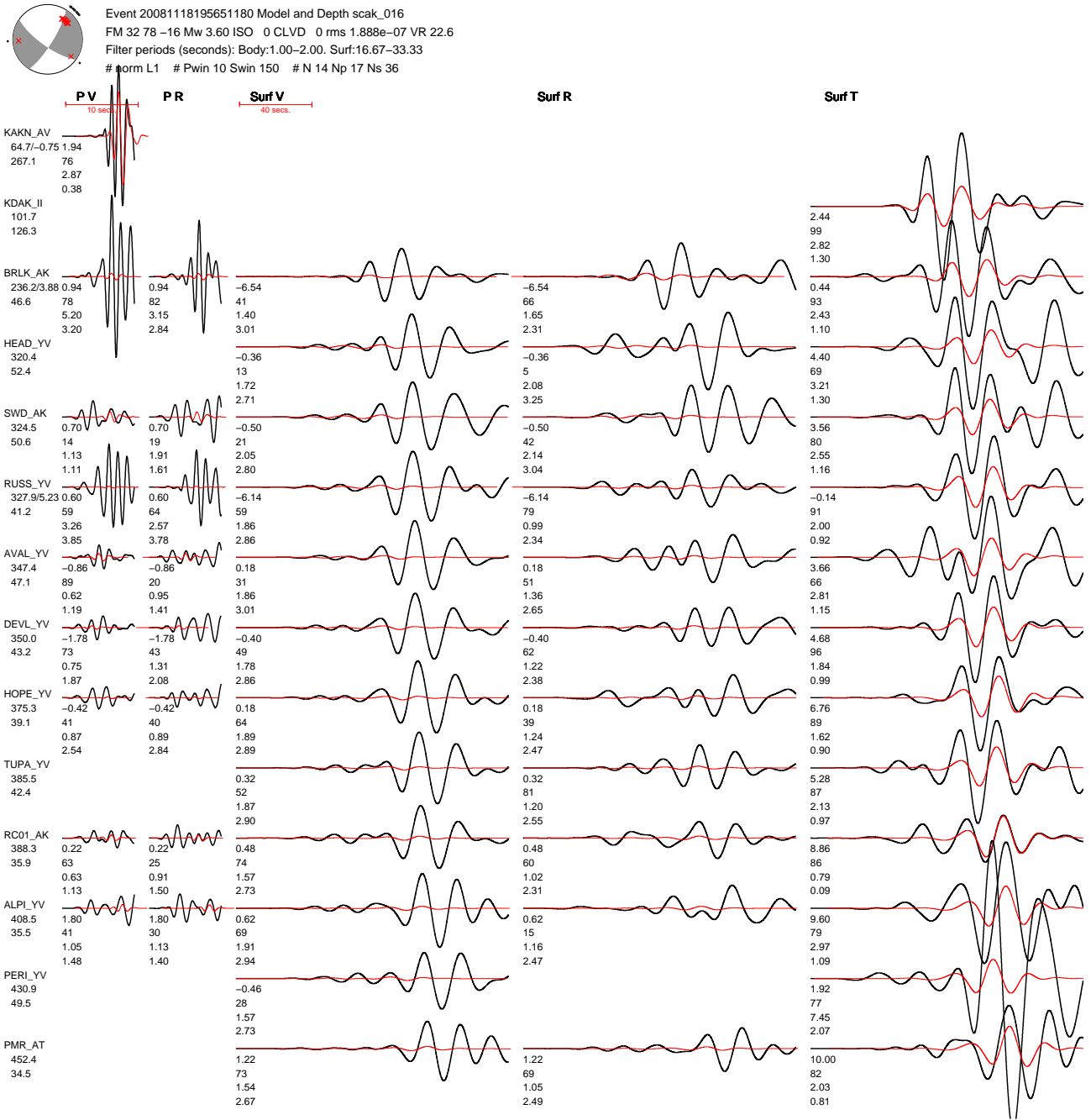


Figure S7: Waveform fits for 20081118195651180 at AEC first-motion solution and at their magnitude estimate (see Figure S6 for waveform fits when allowed to search over magnitude). Smaller amplitude of synthetics shows that the magnitude have been underestimated. The use of long period surface waves for more accurate estimate of magnitude have been known for quite some time now. Magnitude used in this case is M_w 3.6 which is obtained using the first-motion polarity match only, which is much smaller than our estimate of M_w 4 obtained using both the body and surface waves match (see Figure S5).

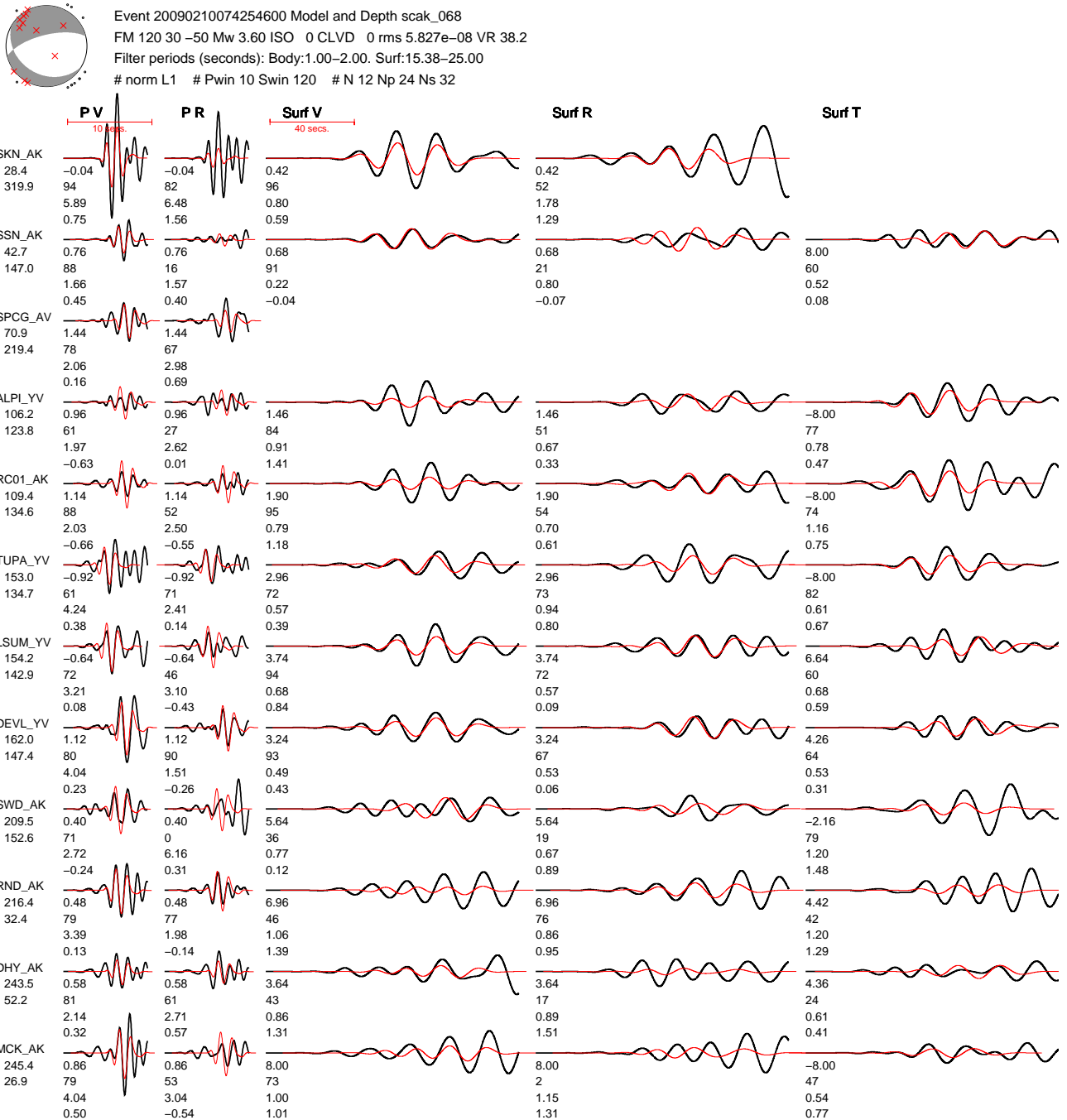


Figure S8: Waveform fits for subset of stations for a small magnitude event (20090210074254600, depth 68 km, M_w 3.6) when inversion is performed using body and surface wave fitting (CAP). Omega difference from AEC first-motion solution (Figure S9) is 68° . See figure header for details about the moment tensor inversion.

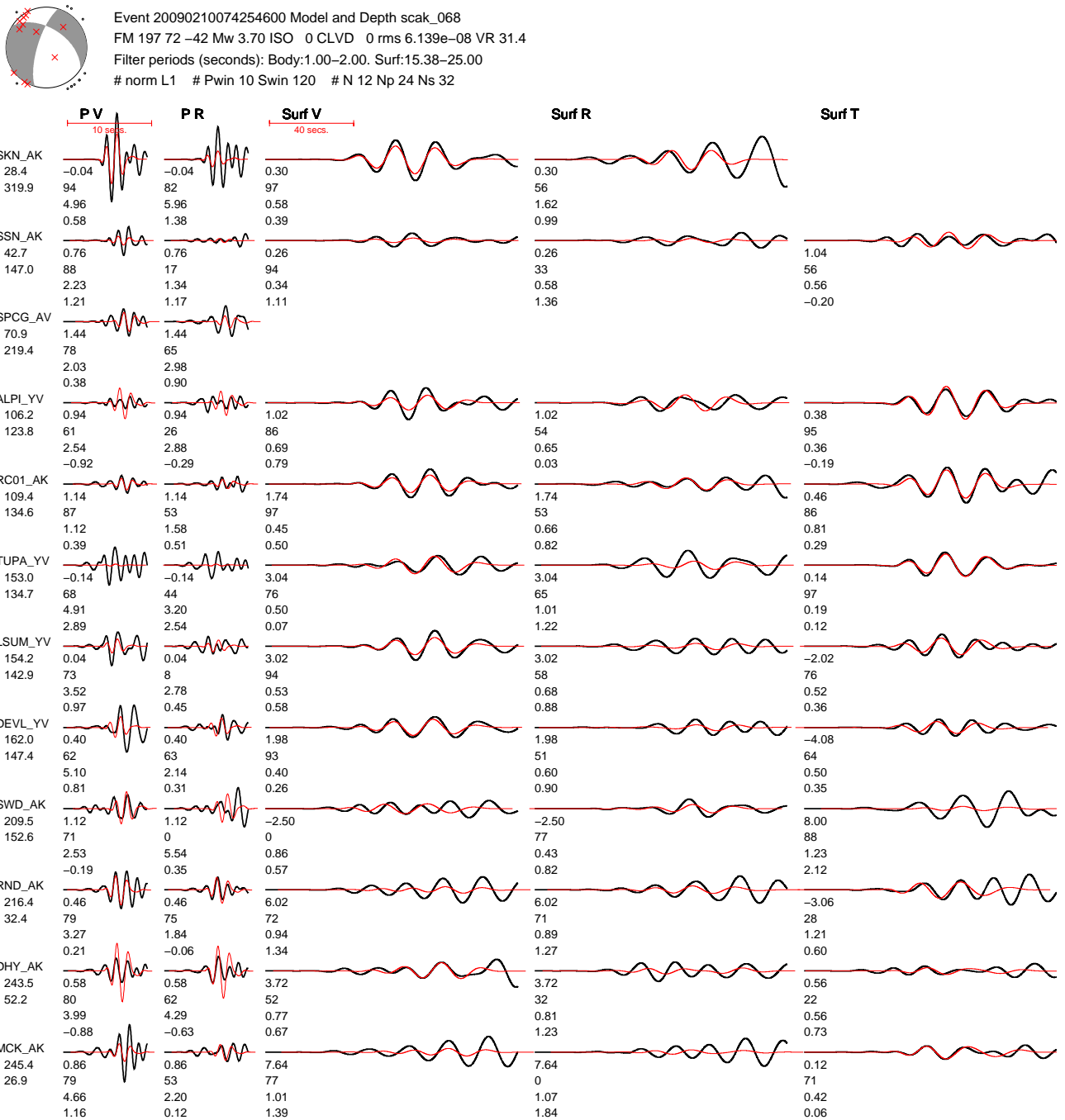


Figure S9: Waveform fits for subset of stations for a small magnitude event 20090210074254600, at AEC first-motion solution and variable magnitude search. The solution used here is obtained using first-motion polarity information only. See Figure S10 for waveform fits when fixed at AEC magnitude, and Figure S8 for our solution obtained from CAP (obtained using body and surface waves). Magnitude obtained in this case is M_w 3.7. See figure header for details about the moment tensor inversion.

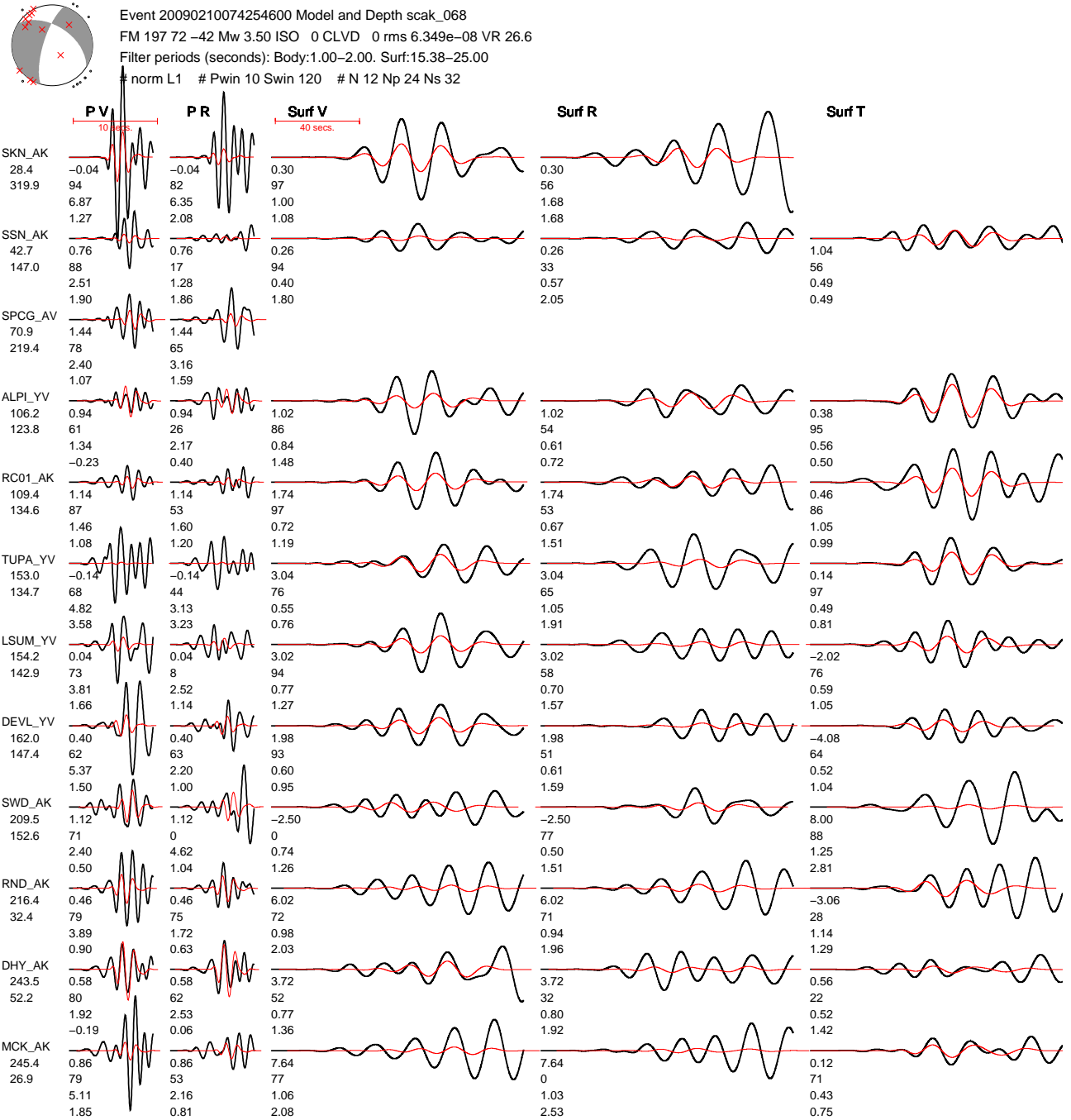


Figure S10: Waveform fits for subset of stations for a small magnitude event 20090210074254600, at AEC first-motion solution and fixed magnitude. See Figure S9 for waveform fits when searching over magnitude, and Figure S8 for our solution obtained from CAP. Magnitude used in this case is M_w 3.5. See figure header for details about the moment tensor inversion.

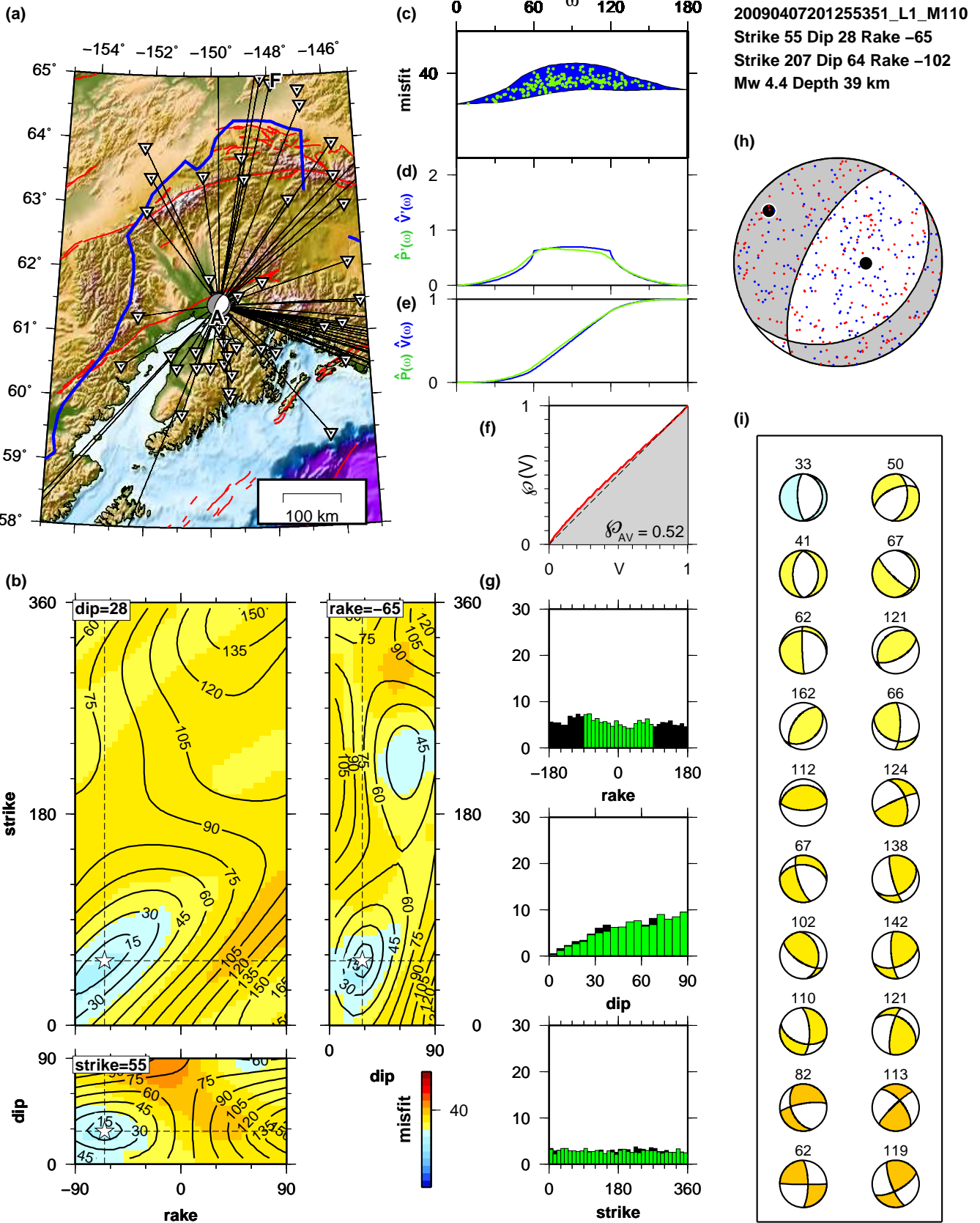


Figure S11: Same as Figure 7, but for a different subset of data (M_{110} ; see Table 1). Each of the six data subset choices is used in Figure 7 (M_{111}) and Figures S11–S15 (M_{110} , M_{011} , M_{101} , M_{112} , M_{012}), respectively.

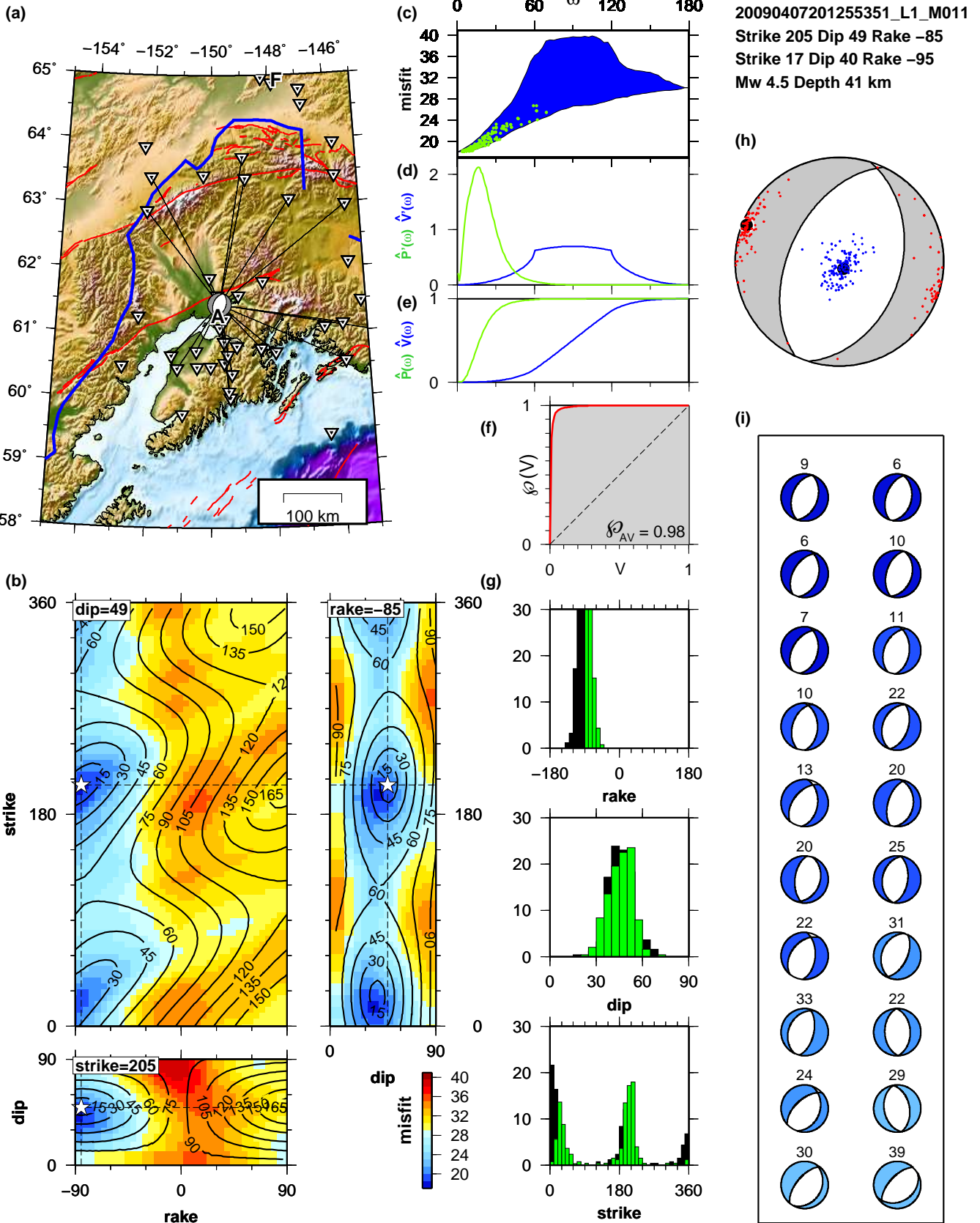


Figure S12: Same as Figure 7, but for a different subset of data (M_{011} ; see Table 1). Each of the six data subset choices is used in Figure 7 (M_{111}) and Figures S11–S15 (M_{110} , M_{011} , M_{101} , M_{112} , M_{012}), respectively.

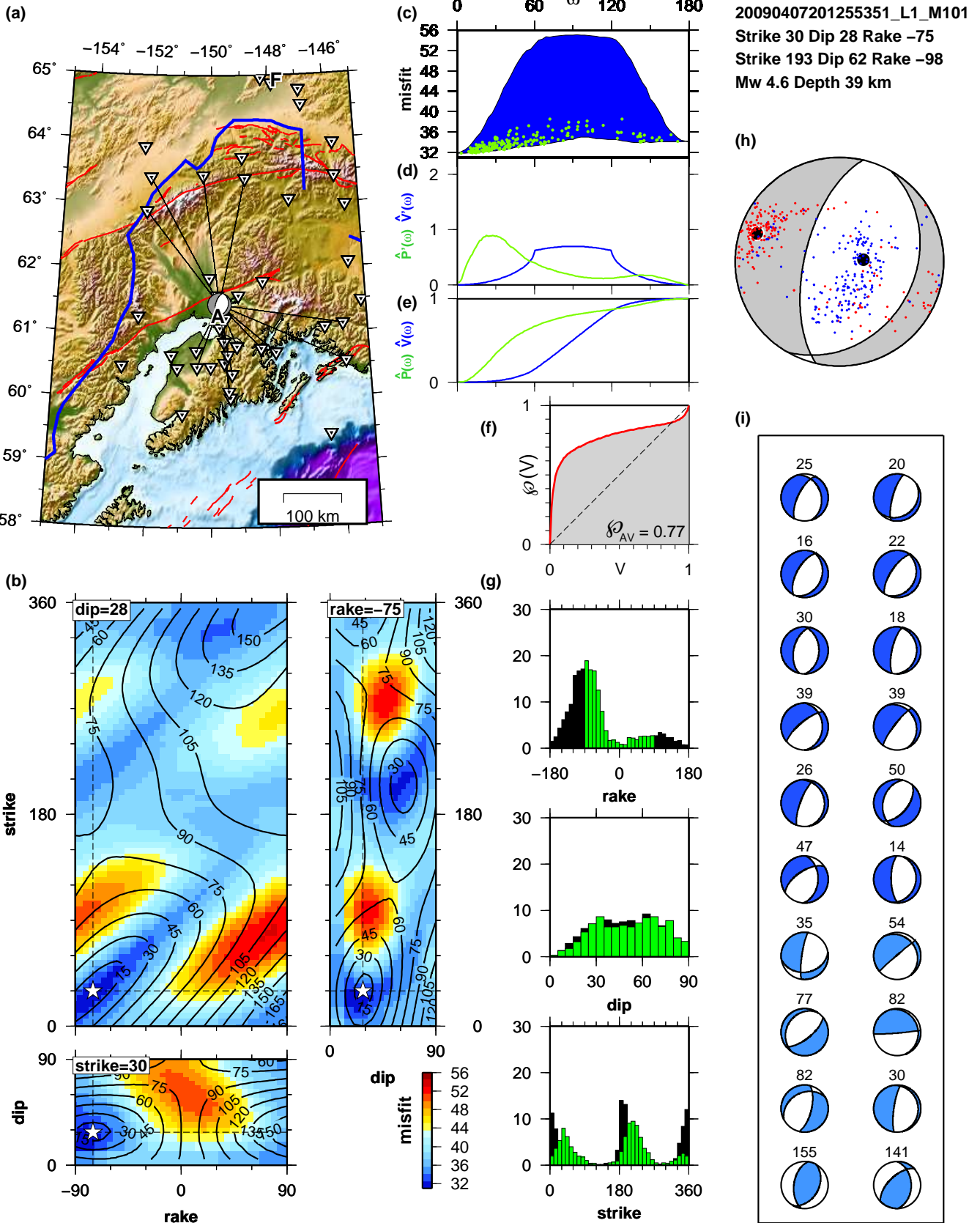


Figure S13: Same as Figure 7, but for a different subset of data (M_{101} ; see Table 1). Each of the six data subset choices is used in Figure 7 (M_{111}) and Figures S11–S15 (M_{110} , M_{011} , M_{101} , M_{112} , M_{012}), respectively.

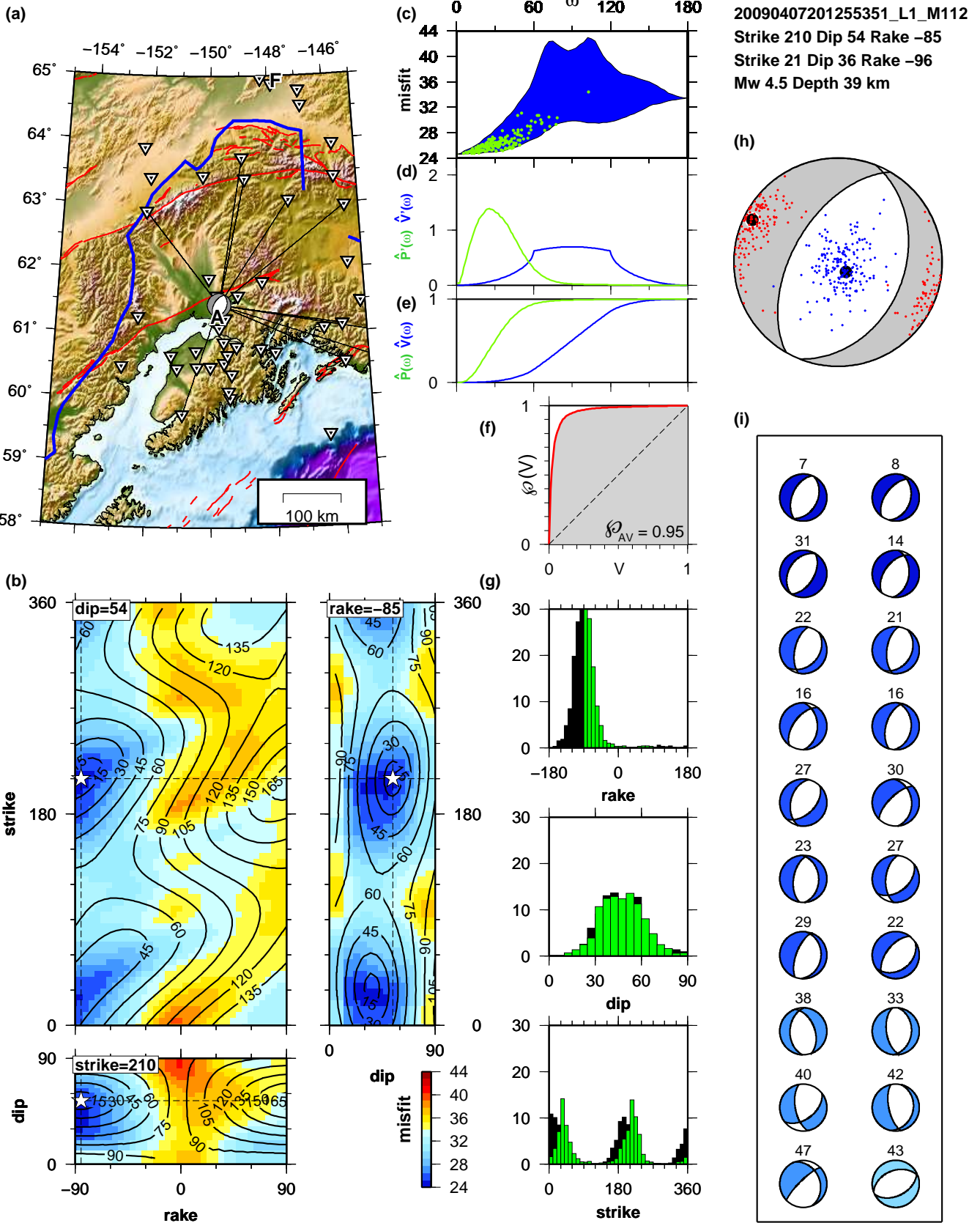


Figure S14: Same as Figure 7, but for a different subset of data (M_{112} ; see Table 1). Each of the six data subset choices is used in Figure 7 (M_{111}) and Figures S11–S15 (M_{110} , M_{011} , M_{101} , M_{112} , M_{012}), respectively.

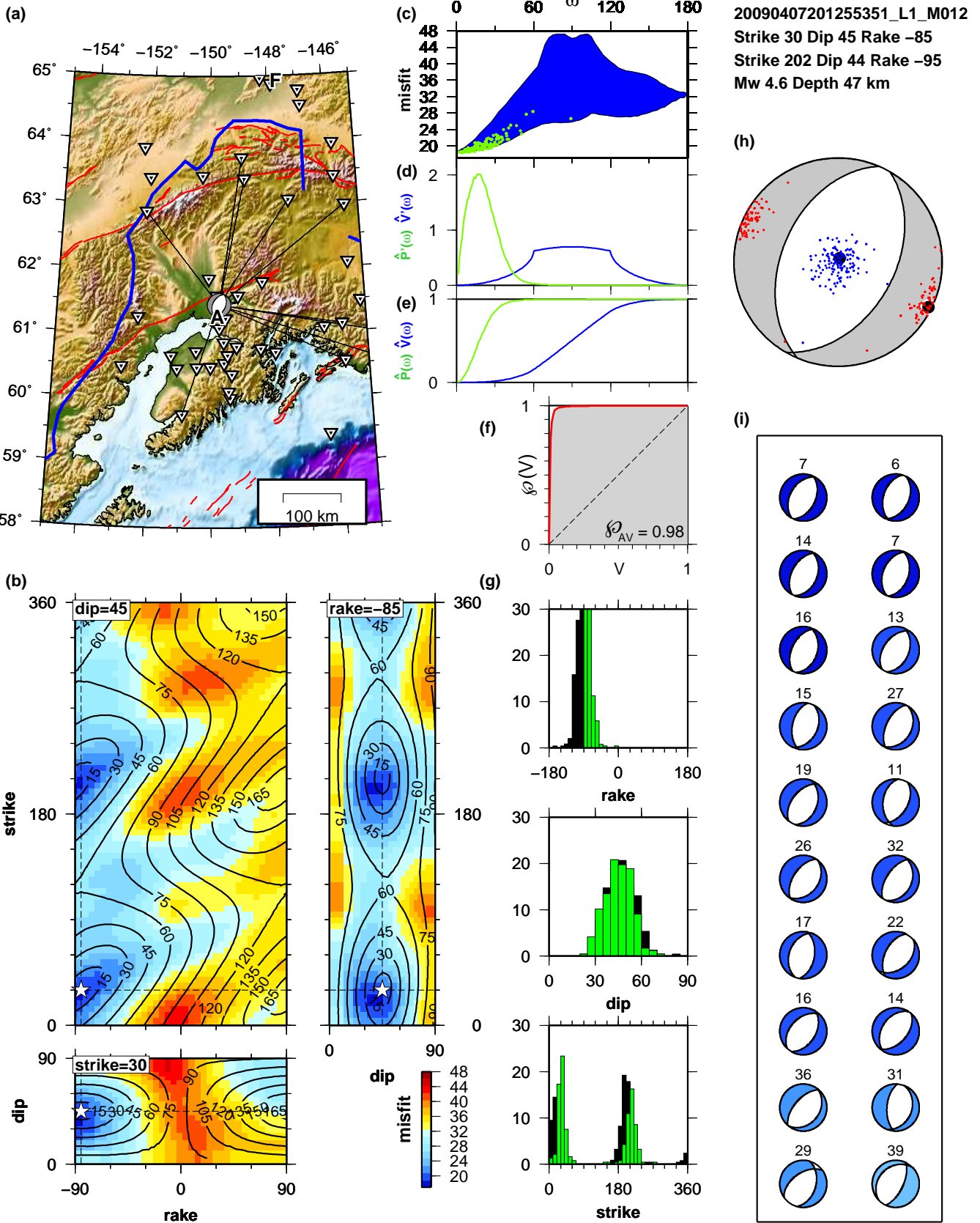


Figure S15: Same as Figure 7, but for a different subset of data (M_{012} ; see Table 1). Each of the six data subset choices is used in Figure 7 (M_{111}) and Figures S11–S15 (M_{110} , M_{011} , M_{101} , M_{112} , M_{012}), respectively.

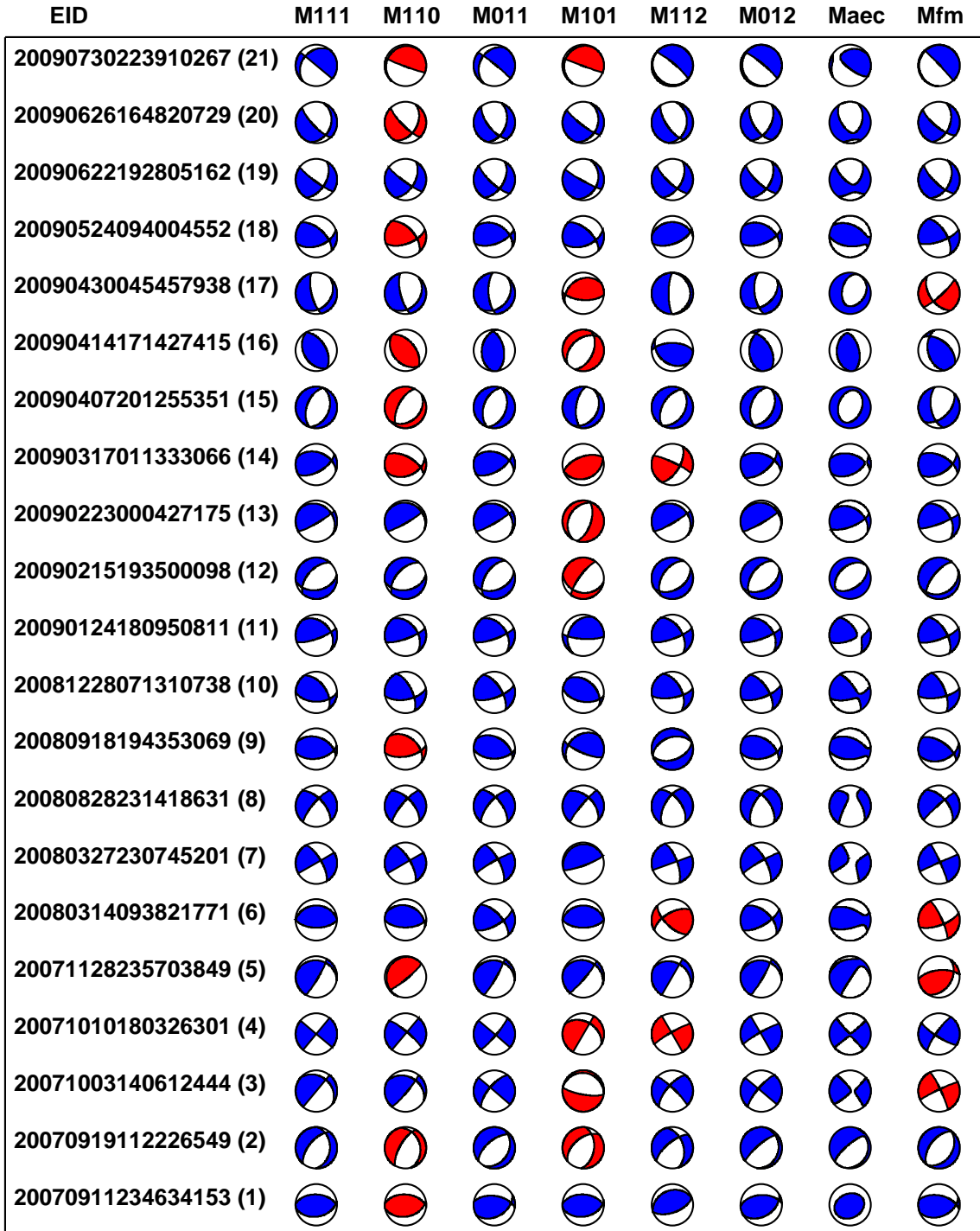


Figure S16: Same as Figure 13 but using the L2 norm instead of the L1 norm. Solutions in the first column should be close to solutions in the first column of Figure 13 since only good stations are used in both cases. A comparison between L1 and L2 results for four cases is shown in Figure 12.

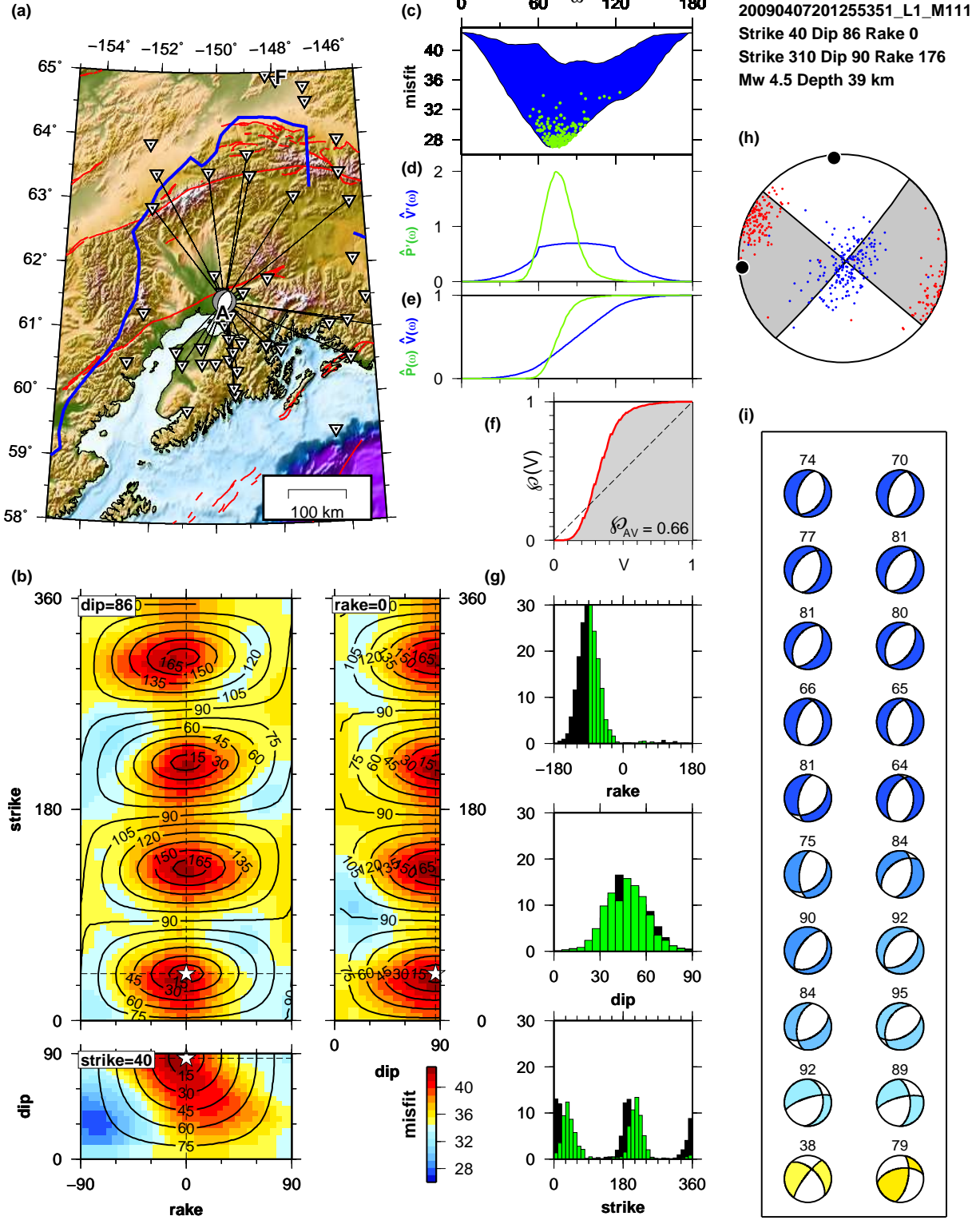


Figure S17: Same as Figure 7, except here we have chosen the reference moment tensor to be the maximum misfit solution M_x rather than the minimum. (a) Beachball for M_x (strike 40° , dip 86° , rake 0°) and $\omega = \angle(M_0, M_x) = 74^\circ$. See Figure 7 for analysis when global minimum M_0 is chosen as M_{ref} , and see Section 7.1 for discussion.

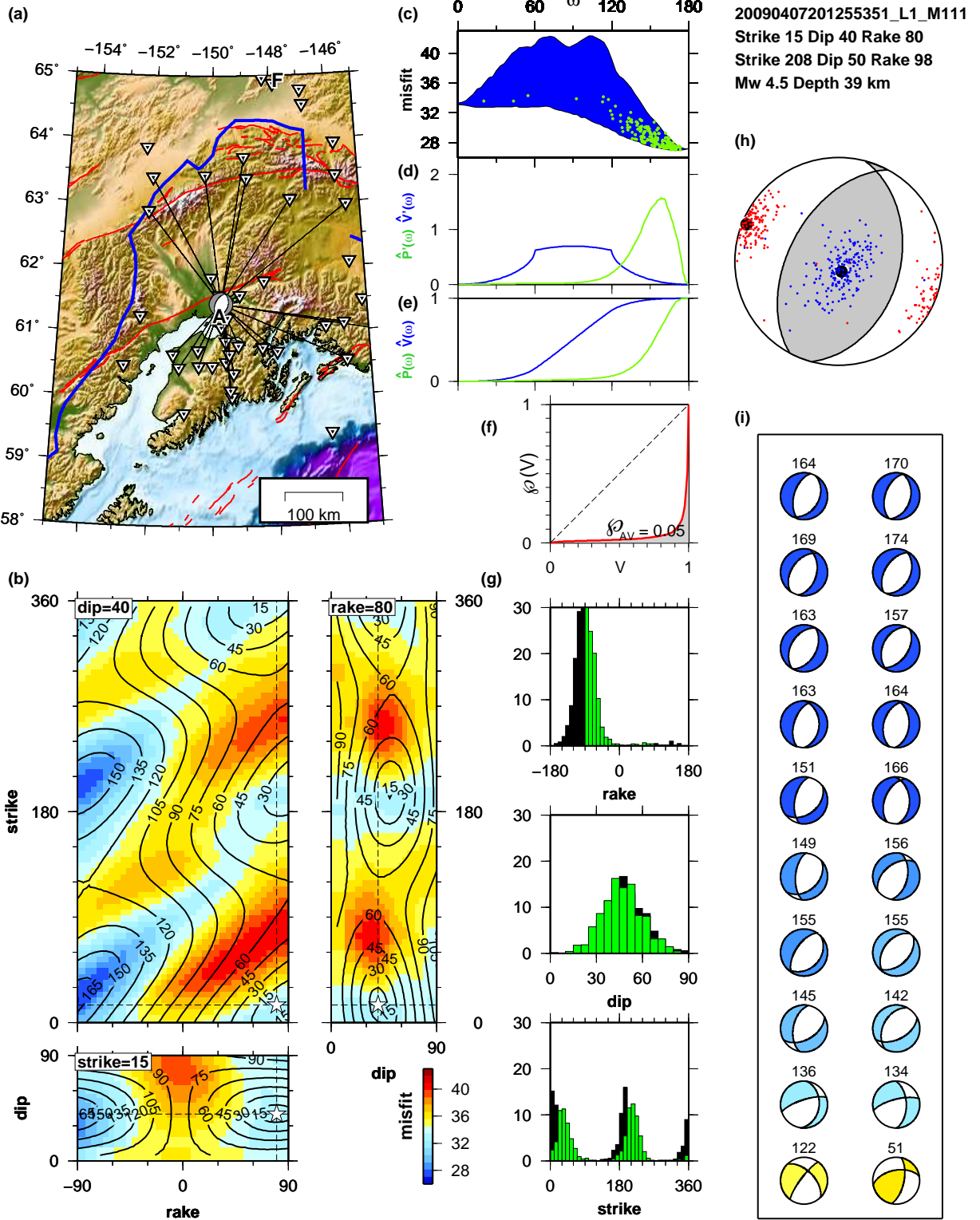


Figure S18: Same as Figure 7, except here we choose the reference moment tensor to be $-M_0$, where M_0 is the best-fitting solution.

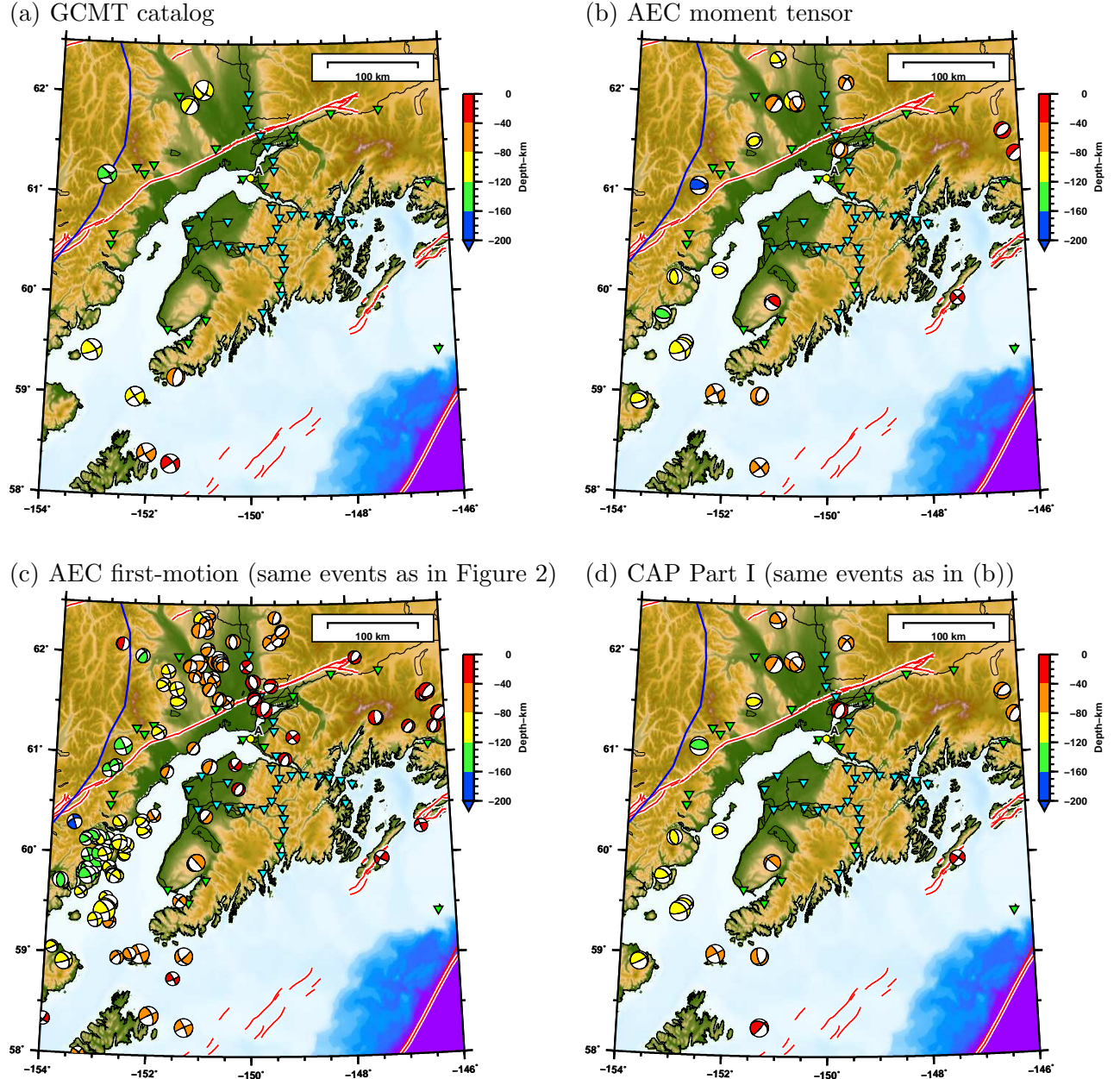


Figure S19: Moment tensor catalogs for the time period of the MOOS deployment (2007-8-15 to 2009-8-15). (a) GCMT catalog (*Ekström et al.*, 2012). (b) AEC moment tensor catalog (21 events: same as Part I catalog) (*Ratchkovski and Hansen*, 2002). (c) Subset of Figure 2 events in the AEC first-motion catalog. Figure 2 shows our moment tensors for the same events. (d) Our moment tensor solutions for the events shown in (b) (Part I catalog).

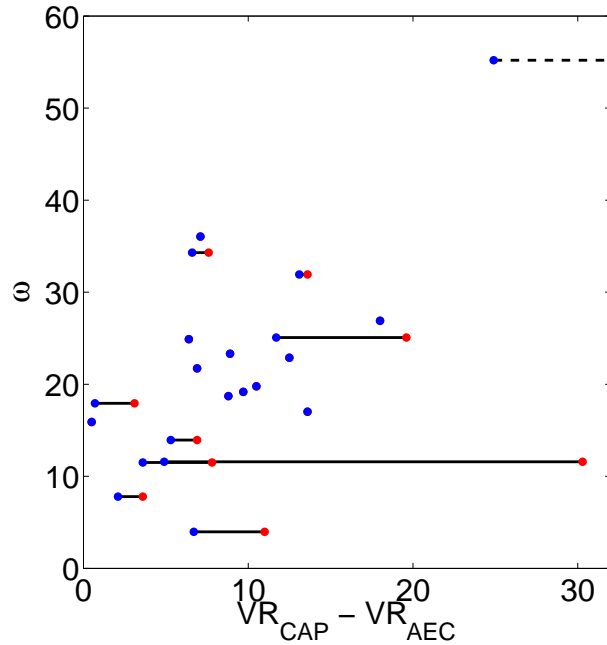


Figure S20: Improvement in waveform fits between our solutions (M_{CAP}) and AEC moment tensor solution (M_{AEC}) for the 21 Part I events, measured in terms of $VR_{\text{CAP}} - VR_{\text{AEC}}$ and $\omega = \angle(M_{\text{CAP}}, M'_{\text{AEC}})$, where the prime notation indicates the closest double couple to M_{AEC} . The improvement in VR for CAP is measured for two separate cases: (red) AEC moment tensor with the AEC magnitude; (blue) AEC moment tensor free to search over magnitude. The blue points are necessarily to the left of (or on top of) the red points. For the highest ω event, 20071003140612444 (uppermost blue point), VR worsens severely when magnitude is fixed; the red point for that event is off the plotting scale at $\Delta VR = 207$.